

## Appendix 5

### Laboratory Works 5 – 2

1. Microscopic observation of Igneous rocks
2. Whole rock chemistry of Igneous rocks
3. K-Ar Dating of Igneous rocks

## 5-2 1. Microscopic Observation of Igneous Rock

### 1-1 Samples

Typical samples of the volcanic rocks collected in the ERZ A by dredge were examined by microscope (Table 1). The microscopic observation was conducted by Dr. Eij Hirano, Geological Laboratory of HIRANO.

Table 1 Sample List of Microscopic Observation

Area	Sampling No.	Depth (m)	No. of Individual Sample	Lithology	Sample No.
ERZ A	04SFAD02	1956-1803	C3	vitric surface of basalt	04SFAD02 TS01
			C5	fragments of quenched	04SFAD02 TS02
	04SFAD03	1954-1801	C5	small pillow or tube	04SFAD03 TS01
			C6	crust of lava flow surface	04SFAD03 TS02
	04SFAD04	1941-1925	C1	fragments of autobrecciated lava	04SFAD04 TS01
			C3	part of pillow lava	04SFAD04 TS02
	04SFAD05	2072-1955	C2	fragments of autobrecciated lava	04SFAD05 TS01
			C5	part of pillow lava	04SFAD05 TS02

### 1-2 Results of Microscopic Observations

The results of microscopic observation are given in Table 2, and descriptions of each hand specimen and thin sections are given at the end of chapter.

### 1-3 Considerations

The samples of 04SFAD02 and 04SFAD03 are clinopyroxene basalt, and samples of 04SFAD04 and 04SFAD05 are, respectively, olivine basalt and aphyric basalt. All of the samples are vitric and abundance of phenocryst is less than 10%. Vesicles are commonly observed, occupying 10 to 30vol%. All the samples are relatively fresh and even slightly altered samples (04SFAD03TS02 and 04SFAD04TS02) only show a small amount of clay in vesicles and along cracks.

The samples of 04SFAD02 and 04SFAD03 have phenocrysts of plagioclase and clinopyroxene, and the groundmass consists of plagioclase and clinopyroxene, in addition to olivine only in 04SFAD03 samples. Opaque minerals (magnetite) are observed only in 04SFAD03TS02. The groundmass olivine does not show reaction rim. Aggregations of acicular (microlite) clinopyroxene and plagioclase of orbicular shape

commonly occur. The samples of 04SFAD03 characteristically show amygdaloidal opaque glass (appearance of microlith).

The samples of 04SFAD04 have plagioclase and olivine phenocrysts with groundmass of plagioclase, olivine and clinopyroxene. Opaque minerals (magnetite) are observed in groundmass of 04SFAD04TS02. The olivine in 04SFAD04 TS01 is acicular crystal, while that of 04SFAD04 TS02 is subhedral to euhedral crystal. Reaction rim is not observed in these samples.

Although 04SFAD05 samples are aphyric, plagioclase phenocrysts are rarely observed. The groundmass, showing texture similar to samples of 04SFAD04, consists of plagioclase, clinopyroxene and magnetite.

Orthopyroxene and silica minerals were not found in any samples and olivine does not show reaction rim. The microscopic observations suggest all samples are silica under-saturated ocean floor basalt.

Table 2 Results of Microscopic Observation

Area	Lithology	Sample No.	Rock Name	Texture	Alteration	Amount of Phenocryst	Phenocryst				Groundmass				Secondary			Remarks
							Pl	Ol	Cpx	Pl	Ol	Cpx	Ap	G	Smc	Si	Goe	
ERZ A	vitric surface of basalt	04SFAD02 TS01	Cpx basalt	Cryptocrystalline e-hyalophitic	not observed	Δ	Δ	-	+	-	-	-	-	⊙	-	-	-	-
	fragments of quenched basalt	04SFAD02 TS02	Cpx basalt	Porphyritic, cryptocrystalline	not observed	Δ	Δ	-	+	-	⊙	-	-	⊙	-	-	-	-
	small pillow or tube	04SFAD03 TS01	Cpx basalt	Cryptocrystalline e-hyalophitic	not observed	Δ	+	-	+	+	○	-	-	⊙	-	-	-	-
	crust of lava flow surface	04SFAD03 TS02	Cpx basalt	Porphyritic, cryptocrystalline	weak	Δ	Δ	-	+	Δ	○	-	-	⊙	Δ	-	-	-
	fragments of autobrecciated lava	04SFAD04 TS01	Ol basalt	Hyalophitic-interstitial	not observed	+	+	+	-	○	⊙	-	-	⊙	-	-	-	Foraminifera, calcite in cavity
	part of pillow lava	04SFAD04 TS02	Ol basalt	Interstitial	weak	Δ	Δ	+	-	○	⊙	Δ	-	⊙	Δ	-	-	Δ
	fragments of autobrecciated lava	04SFAD05 TS01	Aphyric basalt	Hyalophitic	not observed	+	+	-	-	○	○	+	-	⊙	-	-	-	-
	part of pillow lava	04SFAD05 TS02	Aphyric basalt	Hyalophitic	not observed	+	+	-	-	Δ	○	+	-	⊙	-	-	-	-

Amounts (%):  
 ⊙ Dominant (>30)  
 ○ Major (10-30)  
 Δ Minor (3-10)  
 + Trace (<3)

Mineral name:  
 Pl: Plagioclase  
 Ol: Olivine  
 Cpx: Clinopyroxene  
 Oq: Opaque mineral

No1

Sample Number: 01\_04SFAD02-TS01

Rock type: Clinopyroxene basalt

**Naked eye observation:** Glassy surface of dark-colored basalt lava. Magnetism is rarely recognized in the inner part, but is not recognize at the surface.

**Microscopic observation**

Texture: Cryptocrystalline-hyalophitic texture. Transparent glass layer is also recognized. Small amount of plagioclase phenocryst is observed.

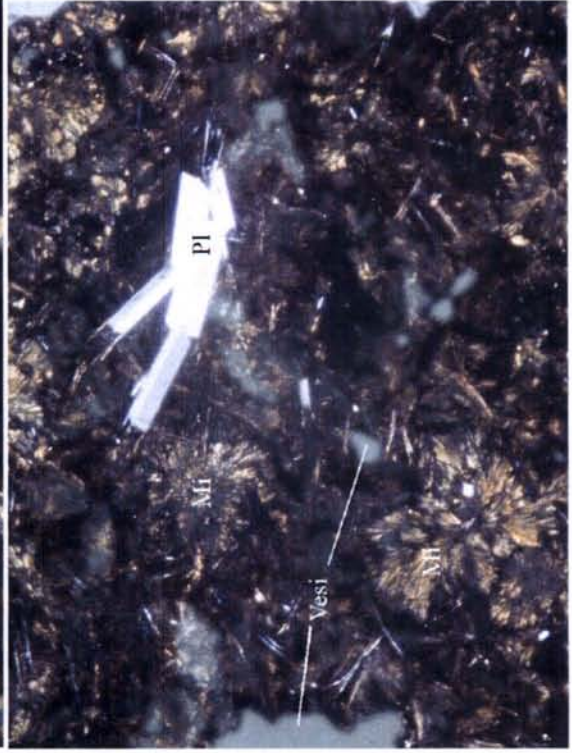
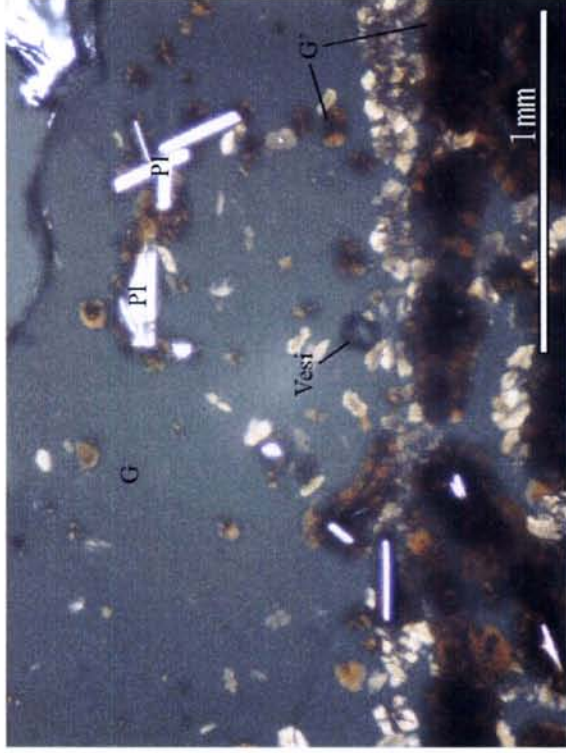
Phenocryst			
Mineral	Texture	Size(mm)	Volume (%)
Plagioclase	prismatic	0.5-3.0	5
Clinopyroxene	short-prismatic	0.6-1.0	<1

Groundmass: Composed of almost turbid glass and clinopyroxene microlite. Vesicle (0.05-0.08mm diameter) is slightly observed.

Groundmass			
Mineral	Texture	Size (mm)	Volume (%)
Clinopyroxene?	fibrous	0.2-0.1 (length)	30
Turbid glass	dark brown		50
Clear glass	pale brown		20

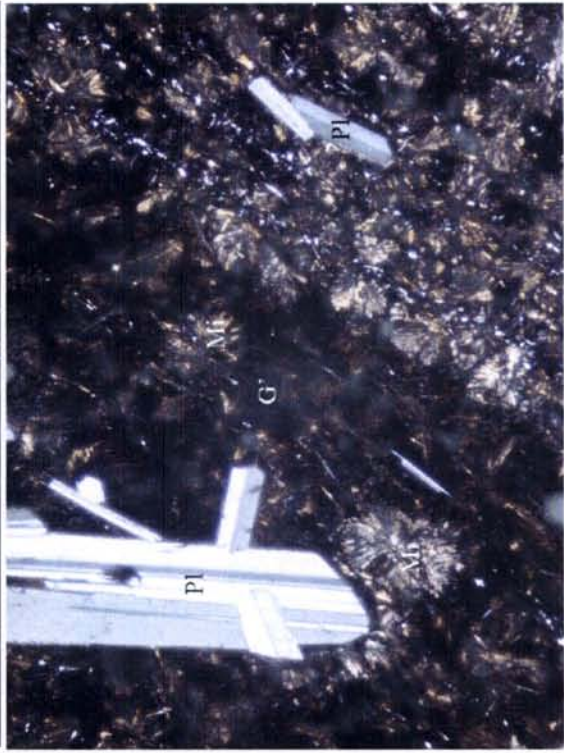
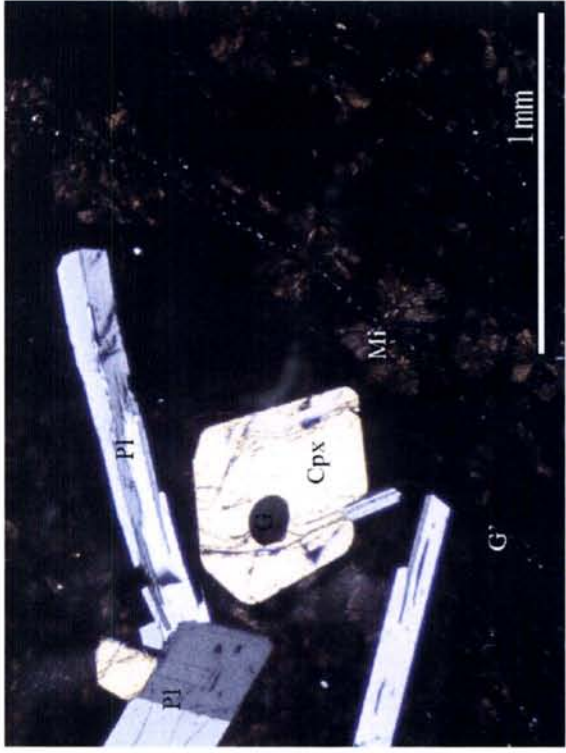
Alteration: Not altered

Alteration			
Mineral	Texture	Size (mm)	Volume (%)



No.2

<p><b>Sample Number:</b> 02_04SFAD02-TS02</p> <p><b>Rock type:</b> Clinopyroxene basalt</p> <p><b>Naked eye observation:</b> Dark-grey, glassy, fine grained and vesicular volcanic rock. Pyroxene and plagioclase phenocryst are scarcely observed. Magnetism is low in fine grained part and quite low in smooth glass part.</p> <p><b>Microscopic observation</b></p> <p>Texture: Porphyritic texture. Turbid glassy - hyaloophitic groundmass. Clear layer with Vidiöle (clinopyroxene microcline) and turbid-dark gray glassy layer makes banded texture. Plagioclase phenocryst is rarely observed.</p>																																	
<p><b>Phenocryst</b></p> <table border="1"> <thead> <tr> <th>Mineral</th> <th>Texture</th> <th>Size(mm)</th> <th>Volume (%)</th> <th>Description</th> </tr> </thead> <tbody> <tr> <td>Clinopyroxene</td> <td>subhedral, prismatic</td> <td>0.5-1.0</td> <td>~1</td> <td>Subophitically including plagioclase. Hollows occupied by glass.</td> </tr> <tr> <td>Plagioclase</td> <td>prismatic</td> <td>0.3-1.5</td> <td>5-10</td> <td>Glomeroporphyritic.</td> </tr> </tbody> </table>				Mineral	Texture	Size(mm)	Volume (%)	Description	Clinopyroxene	subhedral, prismatic	0.5-1.0	~1	Subophitically including plagioclase. Hollows occupied by glass.	Plagioclase	prismatic	0.3-1.5	5-10	Glomeroporphyritic.															
Mineral	Texture	Size(mm)	Volume (%)	Description																													
Clinopyroxene	subhedral, prismatic	0.5-1.0	~1	Subophitically including plagioclase. Hollows occupied by glass.																													
Plagioclase	prismatic	0.3-1.5	5-10	Glomeroporphyritic.																													
<p><b>Groundmass:</b></p> <table border="1"> <thead> <tr> <th>Mineral</th> <th>Texture</th> <th>Size (mm)</th> <th>Volume (%)</th> <th>Description</th> </tr> </thead> <tbody> <tr> <td>Clinopyroxene microcline</td> <td>Feather</td> <td>0.1(length)</td> <td>40</td> <td>Faded-bow-like shape Turbid. Pale brown.</td> </tr> <tr> <td>Plagioclase</td> <td>Acicular</td> <td>0.1(length)</td> <td>10</td> <td>Clear and straight shape microcline</td> </tr> <tr> <td>Magnetite</td> <td>Anchor-like</td> <td>fine grain</td> <td>&lt;1</td> <td>Associating with clinopyroxene.</td> </tr> <tr> <td>Glass</td> <td>Clear-turbid</td> <td>-</td> <td>40-50</td> <td></td> </tr> <tr> <td>Vesicle</td> <td>Formed</td> <td>0.001-0.4</td> <td>1-5</td> <td>Associating with turbid glass or microcline.</td> </tr> </tbody> </table> <p>Alteration: Not altered</p>				Mineral	Texture	Size (mm)	Volume (%)	Description	Clinopyroxene microcline	Feather	0.1(length)	40	Faded-bow-like shape Turbid. Pale brown.	Plagioclase	Acicular	0.1(length)	10	Clear and straight shape microcline	Magnetite	Anchor-like	fine grain	<1	Associating with clinopyroxene.	Glass	Clear-turbid	-	40-50		Vesicle	Formed	0.001-0.4	1-5	Associating with turbid glass or microcline.
Mineral	Texture	Size (mm)	Volume (%)	Description																													
Clinopyroxene microcline	Feather	0.1(length)	40	Faded-bow-like shape Turbid. Pale brown.																													
Plagioclase	Acicular	0.1(length)	10	Clear and straight shape microcline																													
Magnetite	Anchor-like	fine grain	<1	Associating with clinopyroxene.																													
Glass	Clear-turbid	-	40-50																														
Vesicle	Formed	0.001-0.4	1-5	Associating with turbid glass or microcline.																													
<table border="1"> <thead> <tr> <th>Mineral</th> <th>Texture</th> <th>Size (mm)</th> <th>Volume (%)</th> <th>Description</th> </tr> </thead> <tbody> <tr> <td></td> <td></td> <td></td> <td></td> <td></td> </tr> </tbody> </table>				Mineral	Texture	Size (mm)	Volume (%)	Description																									
Mineral	Texture	Size (mm)	Volume (%)	Description																													



No.3

Sample Number:03\_04SFAD03-TS01

Rock type:Clinopyroxene basalt

**Naked eye observation:** Marginal part of pillow or tube. Minor feldspar phenocryst bearing dark-gray fine grained rock with glassy crust (volcanic rock?). Vesicles are abundant in the groundmass. Magnetism is weak at fine grained part and quite weak in clear glass layer.

**Microscopic observation**

**Texture:** Cryptocrystalline to hyalophytic texture. Few pyroxene phenocrysts are observed. Groundmass is composed from glass, acicular feldspar and clinopyroxene microcline. Vesicle are round-irregular shape and occupies about 5 vol% of groundmass

**Phenocryst**

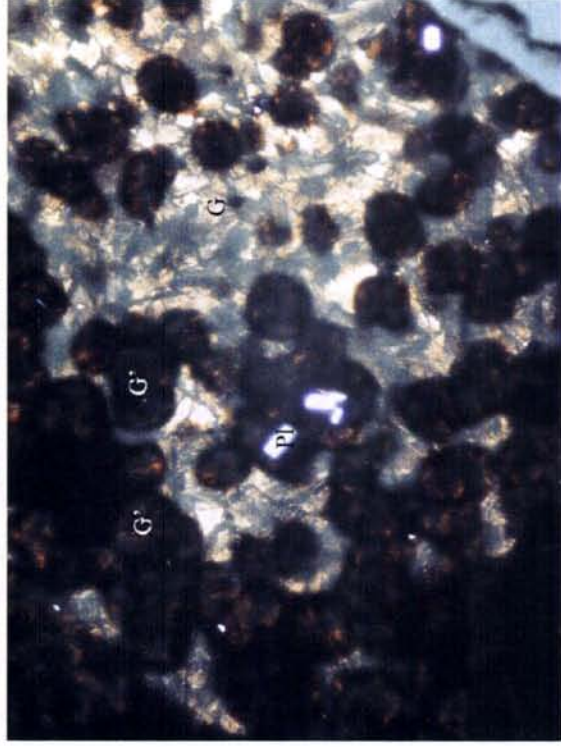
Mineral	Texture	Size(mm)	Volume (%)	Description
Clinopyroxene	subhedral, prismatic	0.5-1.5	2	Including prismatic feldspar.
Plagioclase	prismatic	0.2-1.2	2	Partly glomerophyritic. Irregular edge and hollow are observed.

**Groundmass:** Cryptocrystalline to microcline with minor glassy layer. Acicular plagioclase and round to irregular vesicles are also observed. Vesicles are abundant in microcline rich part.

Mineral	Texture	Size (mm)	Volume (%)	Description
Plagioclase	Acicular-prismatic	~0.2 (length)	~10	
Clinopyroxene	Microcline	~0.2 (length)	30	Feathered, high optical dispersion
Olivine	Granular	0.01	~1	High double refractive index, square or acicular microcline
Glass	Brown, turbid	0.05-1.5	~50	
Vesicle	Rounded, irregular		~5	

Alteration: Not altered

Mineral	Texture	Size (mm)	Volume (%)	Description



No.4

Sample Number:04\_04SFAD03-TS02

Rock type:clinopyroxene basalt

**Naked eye observation:** Crust of the lava surface. Dark gray glassy fine grain volcanic rock (?). Plagioclase phenocryst is observed. Magnetism is weak at fine grained part and quite weak at the glassy part. Partly vesicular.

**Microscopic observation**

Texture: Poplyritic texture and cryptocrystalline in groundmass. Transformation from clear glass to turbid glass by the vitile crystallization is observed. Smectite partly occupies round vesicle.

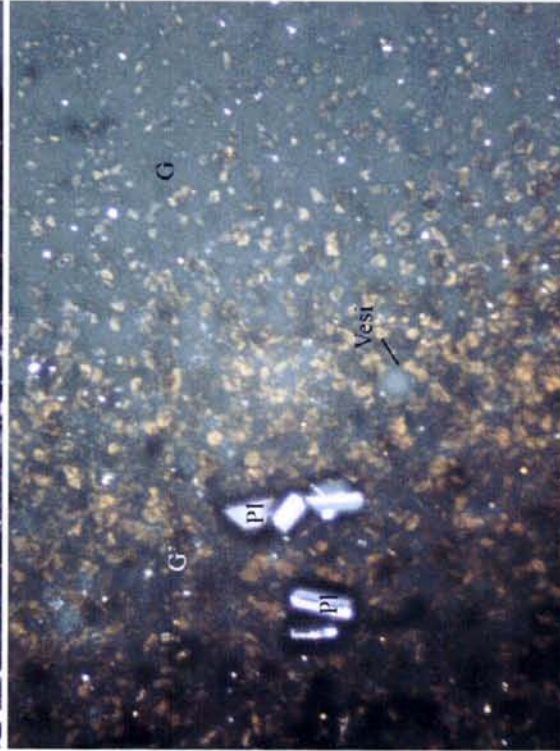
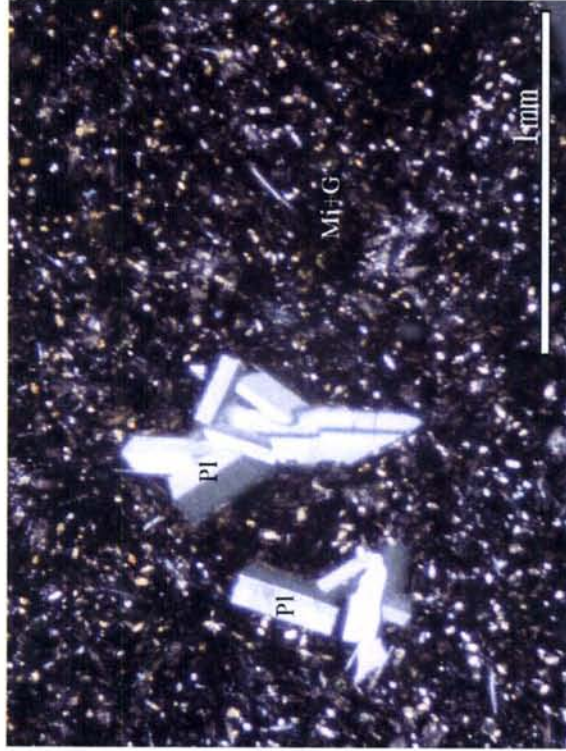
Phenocryst			
Mineral	Texture	Size(mm)	Volume (%)
Plagioclase	Prismatic, tabular	0.1-2.0	5
Clinopyroxene	Short prismatic	0.2-0.4	<1

Groundmass: Except for the glassy part, microcrystalline-cryptocrystalline. Granular olivine, fan-like clinopyroxene and acicular plagioclase are observed.

Groundmass			
Mineral	Texture	Size (mm)	Volume (%)
Clinopyroxene	Fan-like	0.1-0.2	-20
Plagioclase	Acicular	0.1(Length)	-10
Olivine	Granular	0.001	-5
Magnetite	Granular	Micro	-1
Glass	-	-	-50
Vesicular	Oval	0.03-0.2	-5

Alteration: Altered along the fracture. Clay minerals occupy the vesicles.

Alteration			
Mineral	Texture	Size (mm)	Volume (%)
Smectite	Occupying the vesicle	-	-3





No.5

Sample Number:05\_04SFAD04-TS01

Rock type: Olivine basalt

Naked eye observation: Dark gray and fine grained volcanic rock? Aphyric and vesicular. Magnetism is rather high.

**Microscopic observation**

Texture: Hyalophytic-intersertal texture. Little amount of olivine and plagioclase phenocrysts are observed.

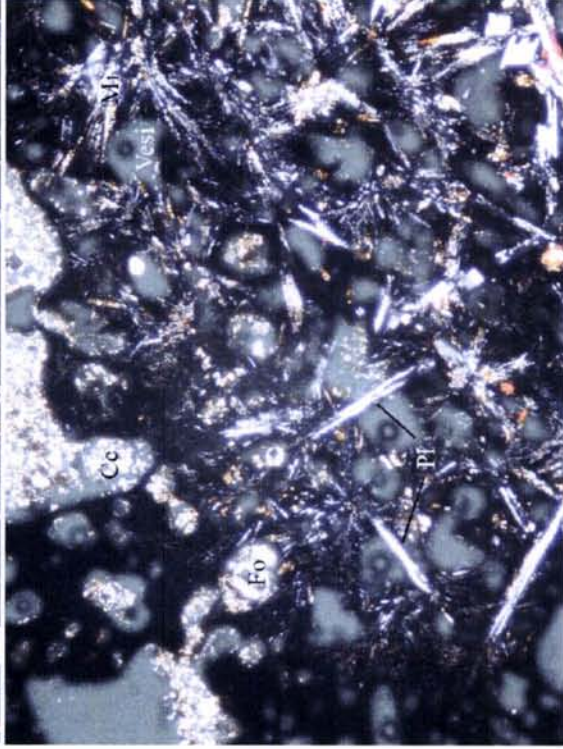
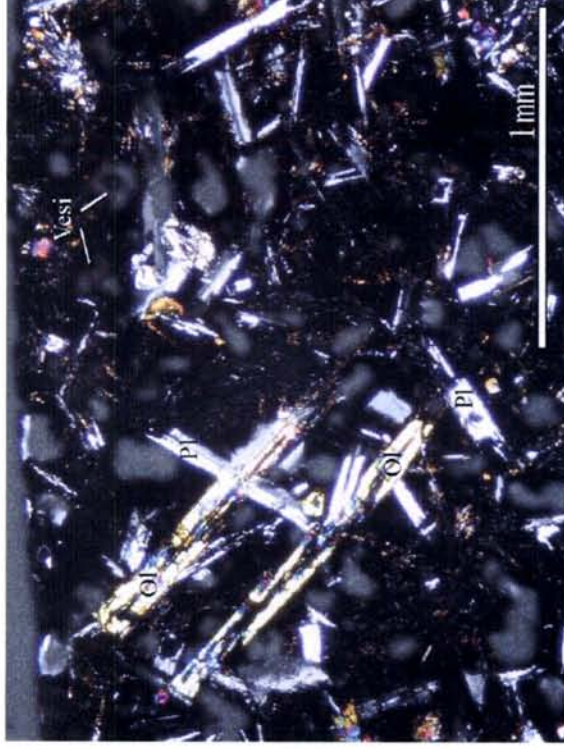
Phenocryst			
Mineral	Texture	Size(mm)	Volume (%)
Olivine	Prismatic	0.2-0.3	-1
Plagioclase	Tabular	0.2-0.3	-1

Groundmass: Hyalophytic-intersertal texture. Most part is composed from turbid glass and vesicles. Vesicles are partly occupied with foraminifera and calcite.

Groundmass			
Mineral	Texture	Size (mm)	Volume (%)
Olivine	Granular, prismatic	0.05-0.2	5
Chloropyroxene	Fan-like	0.05-0.6	-30
Plagioclase	Prismatic	-0.8(Length)	10
Glass	Turbid	-	-30
Calcite	Irregular	-	2
Foraminifera	Rounded	0.05-0.15	-
Vesicle		0.05-0.2	-30

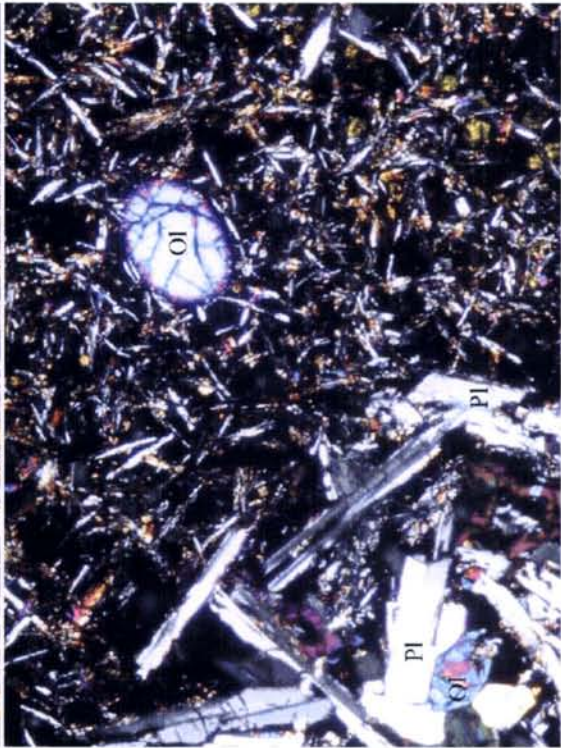
Alteration: Not altered

Alteration			
Mineral	Texture	Size (mm)	Volume (%)



No.6

<p><b>Sample Number:</b> 06_04SFA D04-TS02</p> <p><b>Rock type:</b> olivine basalt</p> <p><b>Naked eye observation:</b> Dark gray, fine grained, homogeneous and vesicular volcanic rock. Small amount of plagioclase phenocryst is recognized. Magnetism is high.</p>																																			
<p><b>Microscopic observation</b></p> <p>Texture: Intersertal texture. Vesicles occupy 10-20% of groundmass and are heterogeneously distributed. Microphenocryst of olivine and plagioclase are observed.</p>																																			
<p><b>Phenocryst</b></p> <table border="1"> <thead> <tr> <th>Mineral</th> <th>Texture</th> <th>Size(mm)</th> <th>Volume (%)</th> <th>Description</th> </tr> </thead> <tbody> <tr> <td>Olivine</td> <td>Prismatic, evo</td> <td>0.3-0.5</td> <td>~2</td> <td>Many crystals are skeletal.</td> </tr> <tr> <td>Plagioclase</td> <td>Prismatic</td> <td>0.6</td> <td>~3</td> <td>Partly included by olivine.</td> </tr> </tbody> </table>				Mineral	Texture	Size(mm)	Volume (%)	Description	Olivine	Prismatic, evo	0.3-0.5	~2	Many crystals are skeletal.	Plagioclase	Prismatic	0.6	~3	Partly included by olivine.																	
Mineral	Texture	Size(mm)	Volume (%)	Description																															
Olivine	Prismatic, evo	0.3-0.5	~2	Many crystals are skeletal.																															
Plagioclase	Prismatic	0.6	~3	Partly included by olivine.																															
<p><b>Groundmass:</b> Intersertal texture. Mainly composed of plagioclase lath, fan-like clinopyroxene and turbid glass.</p> <table border="1"> <thead> <tr> <th>Mineral</th> <th>Texture</th> <th>Size (mm)</th> <th>Volume (%)</th> <th>Description</th> </tr> </thead> <tbody> <tr> <td>Olivine</td> <td>Granular</td> <td>0.02-0.2</td> <td>~2</td> <td rowspan="2">Fan-like microlite and clear crystal. Many shows swallow-tail shape.</td> </tr> <tr> <td>Clinopyroxene</td> <td>Prismatic</td> <td>0.05-0.2</td> <td>~30</td> </tr> <tr> <td>Plagioclase</td> <td>Prismatic-ao lath</td> <td>0.2-0.5</td> <td>10</td> <td rowspan="2">Associating with glass and clinopyroxene. Dark brown and turbid.</td> </tr> <tr> <td>Magnetite</td> <td>Dendritic</td> <td>0.002</td> <td>5</td> </tr> <tr> <td>Glass</td> <td>Turbid</td> <td>-</td> <td>~40</td> <td rowspan="2">Occupying vesicle.</td> </tr> <tr> <td>Vesicle</td> <td>Rounded-ir egular</td> <td>0.2-0.4</td> <td>10-20</td> </tr> </tbody> </table>				Mineral	Texture	Size (mm)	Volume (%)	Description	Olivine	Granular	0.02-0.2	~2	Fan-like microlite and clear crystal. Many shows swallow-tail shape.	Clinopyroxene	Prismatic	0.05-0.2	~30	Plagioclase	Prismatic-ao lath	0.2-0.5	10	Associating with glass and clinopyroxene. Dark brown and turbid.	Magnetite	Dendritic	0.002	5	Glass	Turbid	-	~40	Occupying vesicle.	Vesicle	Rounded-ir egular	0.2-0.4	10-20
Mineral	Texture	Size (mm)	Volume (%)	Description																															
Olivine	Granular	0.02-0.2	~2	Fan-like microlite and clear crystal. Many shows swallow-tail shape.																															
Clinopyroxene	Prismatic	0.05-0.2	~30																																
Plagioclase	Prismatic-ao lath	0.2-0.5	10	Associating with glass and clinopyroxene. Dark brown and turbid.																															
Magnetite	Dendritic	0.002	5																																
Glass	Turbid	-	~40	Occupying vesicle.																															
Vesicle	Rounded-ir egular	0.2-0.4	10-20																																
<p><b>Alteration:</b> Clay minerals and goethite partly occupying vesicle</p> <table border="1"> <thead> <tr> <th>Mineral</th> <th>Texture</th> <th>Size (mm)</th> <th>Volume (%)</th> <th>Description</th> </tr> </thead> <tbody> <tr> <td>Smectite</td> <td>Film</td> <td>0.05 (Thickness)</td> <td>~5</td> <td rowspan="2">Deep yellow. Formed along vesicle inner wall. Optically positive. Red. Showing narrow birefringence.</td> </tr> <tr> <td>Goethite</td> <td>Tabular</td> <td>0.1-0.6</td> <td>~5</td> </tr> </tbody> </table>				Mineral	Texture	Size (mm)	Volume (%)	Description	Smectite	Film	0.05 (Thickness)	~5	Deep yellow. Formed along vesicle inner wall. Optically positive. Red. Showing narrow birefringence.	Goethite	Tabular	0.1-0.6	~5																		
Mineral	Texture	Size (mm)	Volume (%)	Description																															
Smectite	Film	0.05 (Thickness)	~5	Deep yellow. Formed along vesicle inner wall. Optically positive. Red. Showing narrow birefringence.																															
Goethite	Tabular	0.1-0.6	~5																																



No.7

Sample Number:07\_04SEAD05-TS01

Rock type:Aphyric basalt

Naked eye observation: Dark gray, fine grained, homogeneous and vesicular volcanic rock. Small amount of plagioclase phenocryst is recognized Magnetism is high.

**Microscopic observation**

Texture: Hyaloophitic texture. Vesicles occupy 30% of groundmass.

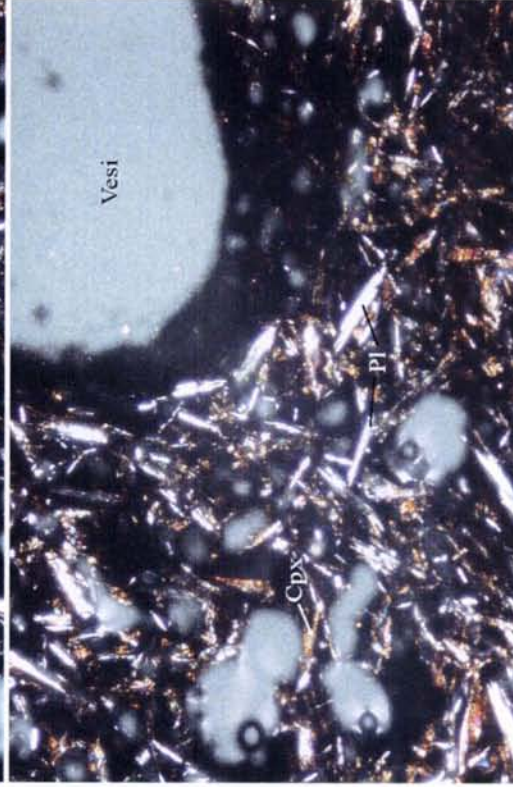
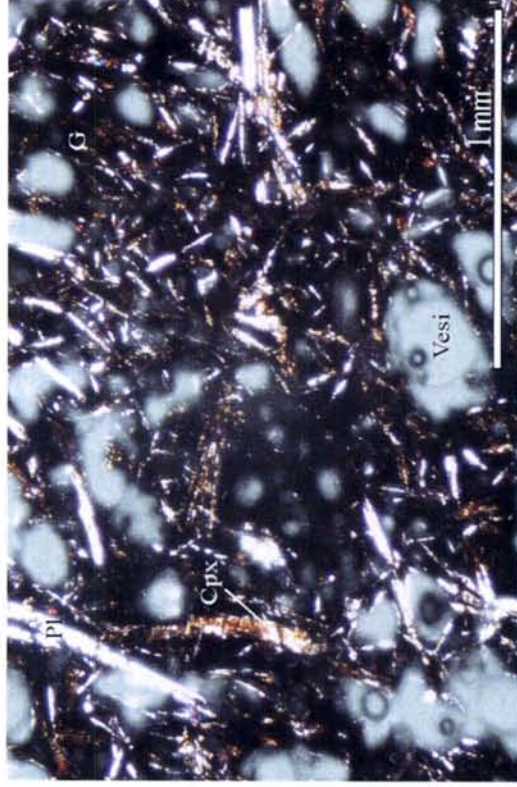
Phenocryst				
Mineral	Texture	Size(mm)	Volume (%)	Description
Plagioclase	Prismatic	0.6(Length)	~2	Thin, Irregular edge. Swallow-tail shape.

Groundmass: Mainly composed from brown turbid glass with microilite(clinopyroxene) and acicular plagioclase. Vesicular.

Mineral	Texture	Size (mm)	Volume (%)	Description
Plagioclase	Acicular, prismatic	~0.3(Length)	10	Edge of crystal is swallow-tail shape.
Clinopyroxene	Fan-like	~0.4(Length)	20	Microilite. Thin acicular
Glass	Turbid		40-50	Brown. Turbid
Magnetite	Dendritic	Micro	<2	Associating with clinopyroxene. Also formed along plagioclase rim.
Vesicle	Irregular	0.1-2.0	20-30	Variable size. Irregular.

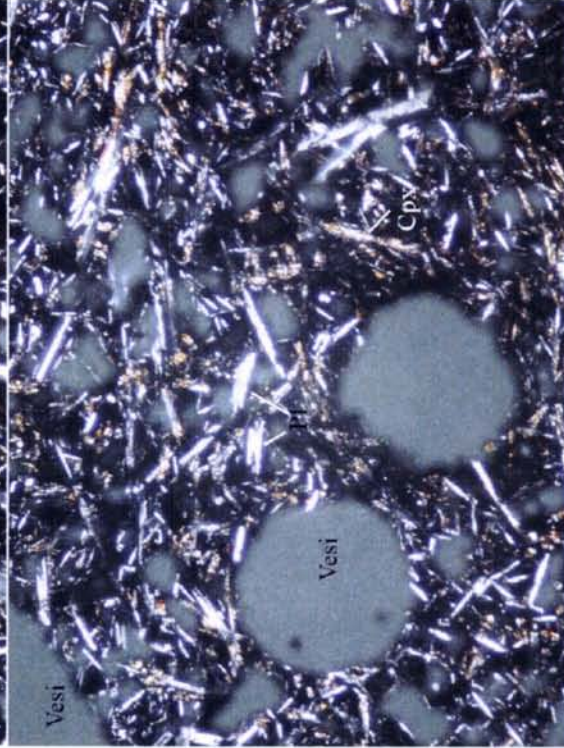
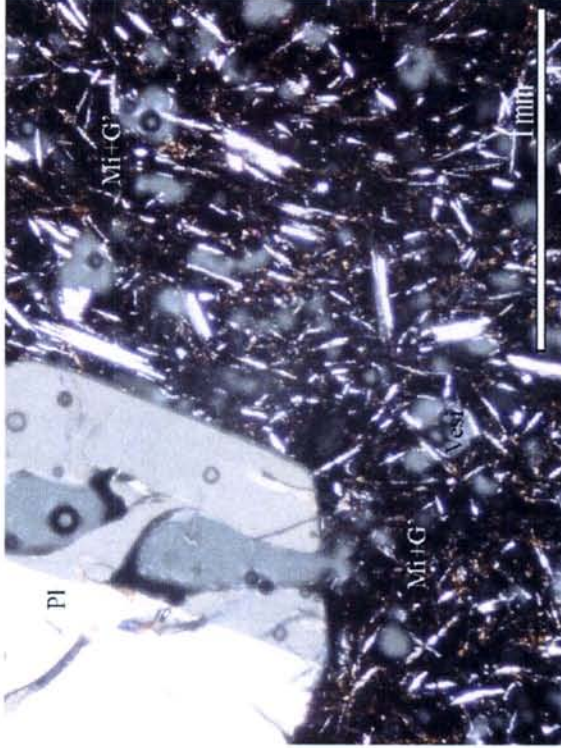
Alteration: Not altered

Mineral	Texture	Size (mm)	Volume (%)	Description



No.8

<p><b>Sample Number:</b>08_04SFAD05-TS02</p> <p><b>Rock type:</b>Aphyric basalt</p> <p><b>Naked eye observation:</b> Dark gray, fine grained, homogeneous and vesicular volcanic rock. Small amount of plagioclase phenocryst is recognized. Magnetism is high.</p> <p><b>Microscopic observation</b></p> <p>Texture: Hyaloclitic texture. Mainly composed from turbid glass with microilite (clinopyroxene) and acicular plagioclase. Vesicular.</p>																																											
<p><b>Phenocryst</b></p> <table border="1"> <thead> <tr> <th>Mineral</th> <th>Texture</th> <th>Size(mm)</th> <th>Volume (%)</th> <th>Description</th> </tr> </thead> <tbody> <tr> <td>Plagioclase</td> <td>Prismatic</td> <td>2.5</td> <td>&lt;1</td> <td>Only one hollow crystal is observed. Subhedral and acicular.</td> </tr> </tbody> </table>				Mineral	Texture	Size(mm)	Volume (%)	Description	Plagioclase	Prismatic	2.5	<1	Only one hollow crystal is observed. Subhedral and acicular.																														
Mineral	Texture	Size(mm)	Volume (%)	Description																																							
Plagioclase	Prismatic	2.5	<1	Only one hollow crystal is observed. Subhedral and acicular.																																							
<p><b>Groundmass:</b> Mainly composed from brown turbid glass with microilite(clinopyroxene) and acicular plagioclase.</p> <table border="1"> <thead> <tr> <th>Mineral</th> <th>Texture</th> <th>Size (mm)</th> <th>Volume (%)</th> <th>Description</th> </tr> </thead> <tbody> <tr> <td>Plagioclase</td> <td>Acicular</td> <td>0.2(L.Length)</td> <td>10</td> <td>Edge of crystal is swallow-tail shape</td> </tr> <tr> <td>Clinopyroxene</td> <td>Fan-like</td> <td>0.2(L.Length)</td> <td>20</td> <td>High optical dispersion and oblique extinction.</td> </tr> <tr> <td>Magnetite</td> <td>Dendritic</td> <td>Micro</td> <td>&lt;1</td> <td>Crystallizing along clinopyroxene microilite surface. Dendritic.</td> </tr> <tr> <td>Glass</td> <td>Turbid</td> <td>-</td> <td>40</td> <td>Turbid. Brown.</td> </tr> <tr> <td>Vesicle</td> <td>Oval-irregular</td> <td>0.05-2.0</td> <td>20-30</td> <td>Small oval type (&lt;0.1mm in diameter) and trigonal type (1.2mm in diameter)</td> </tr> </tbody> </table> <p>Alteration: Not altered</p> <table border="1"> <thead> <tr> <th>Mineral</th> <th>Texture</th> <th>Size (mm)</th> <th>Volume (%)</th> <th>Description</th> </tr> </thead> <tbody> <tr> <td></td> <td></td> <td></td> <td></td> <td></td> </tr> </tbody> </table>				Mineral	Texture	Size (mm)	Volume (%)	Description	Plagioclase	Acicular	0.2(L.Length)	10	Edge of crystal is swallow-tail shape	Clinopyroxene	Fan-like	0.2(L.Length)	20	High optical dispersion and oblique extinction.	Magnetite	Dendritic	Micro	<1	Crystallizing along clinopyroxene microilite surface. Dendritic.	Glass	Turbid	-	40	Turbid. Brown.	Vesicle	Oval-irregular	0.05-2.0	20-30	Small oval type (<0.1mm in diameter) and trigonal type (1.2mm in diameter)	Mineral	Texture	Size (mm)	Volume (%)	Description					
Mineral	Texture	Size (mm)	Volume (%)	Description																																							
Plagioclase	Acicular	0.2(L.Length)	10	Edge of crystal is swallow-tail shape																																							
Clinopyroxene	Fan-like	0.2(L.Length)	20	High optical dispersion and oblique extinction.																																							
Magnetite	Dendritic	Micro	<1	Crystallizing along clinopyroxene microilite surface. Dendritic.																																							
Glass	Turbid	-	40	Turbid. Brown.																																							
Vesicle	Oval-irregular	0.05-2.0	20-30	Small oval type (<0.1mm in diameter) and trigonal type (1.2mm in diameter)																																							
Mineral	Texture	Size (mm)	Volume (%)	Description																																							



## 5-2 2. Whole Rock Chemistry of Igneous Rocks

### 2-1 Samples

Whole rock chemical analyses were conducted for volcanic rocks using the same samples as microscopic observations (Table 1).

Table 1 Rock Samples for Chemical Analyses

Area	Sampling No.	Depth (m)	No. of Individual Sample	Lithology	Sample No.
ERZ A	04SFAD02	1956-1803	C3	vitric surface of basalt	04SFAD02 CA01
			C5	fragments of quenched basalt	04SFAD02 CA02
	04SFAD03	1954-1801	C5	small pillow or tube	04SFAD03 CA01
			C6	crust of lava flow surface	04SFAD03 CA02
	04SFAD04	1941-1925	C1	fragments of autobrecciated	04SFAD04 CA01
			C3	part of pillow lava	04SFAD04 CA02
	04SFAD05	2072-1955	C2	fragments of autobrecciated	04SFAD05 CA01
			C5	part of pillow lava	04SFAD05 CA02

### 2-2 Analyzed Elements and Analytical Methods

A total of 44 elements, including major elements, trace elements and REE, were analyzed for whole rock chemical analyses. Analytical elements, analytical methods and detection limits are given on Tables 2. The chemical analyses were conducted at ALS Chemex, Canada. Before the chemical analyses desalination of the samples were conducted by supersonic washer using the deionized water for twenty four hours, repeating three times.

Table 2 Analytical Methods and Analyzed Elements

Analyzed Elements (lower limit-upper limit)	Analytical Method
SiO <sub>2</sub> , TiO <sub>2</sub> , Al <sub>2</sub> O <sub>3</sub> , Fe <sub>2</sub> O <sub>3</sub> , MnO, MgO, CaO, Na <sub>2</sub> O, K <sub>2</sub> O, P <sub>2</sub> O <sub>5</sub> (0.01-100%)	ICP-AES
FeO (0.1-100%)	Titration
H <sub>2</sub> O <sup>+</sup> (0.1-100%), H <sub>2</sub> O <sup>-</sup> (0.1-100%)	Gravitational Method
CO <sub>2</sub> (0.05-100%)	LECO
LOI (0.01-100%)	After fusing at 1000 deg.C gravitationally determined
Rb (0.2ppm- ), Ba (1ppm-), Zr (1ppm- ), Cs (0.05ppm- ), Y, Ta, U (0.1ppm- )	ICP-MS
Sr (0.2ppm- ), V (1ppm- ), Nb, Hf, Th (0.1ppm- ), Pb, Ni (0.5ppm- )	
Pr, Sm, Gd, Dy, Tb, Ho, Er, Yb, Eu, Tm, Lu (0.01ppm- )	

### 2-3 Analytical Results

The results of chemical analyses are shown on Table 3.

Table 3 Results of Whole rock Chemical Analyses

Area	Sampling No.	Depth (m)	No. of Individual Sample	Lithology	Sample No.	SiO <sub>2</sub>	TiO <sub>2</sub>	Al <sub>2</sub> O <sub>3</sub>	FeO	Fe <sub>2</sub> O <sub>3</sub>	MnO	MgO	CaO	Na <sub>2</sub> O	K <sub>2</sub> O	P <sub>2</sub> O <sub>5</sub>	LOI	Total	H <sub>2</sub> O*	H <sub>2</sub> O	CO <sub>2</sub>	FeO*	Mg#		
						%	%	%	%	%	%	%	%	%	%	%	%	%	%	%	%	%	%	%	
ERZ A	04SFAD02	1954-1803	C3	vitric surface of basalt	04SFAD02 CA01	50.12	1.421	14.04	9.32	1.77	0.197	7.39	11.49	2.62	0.09	0.12	1.23	99.81	0.20	0.77	<d.l.	10.91	0.55		
	04SFAD02	1954-1803	C5	Fragments of quenched basalt	04SFAD02 CA02	50.21	1.446	13.99	9.47	1.88	0.192	7.33	11.42	2.63	0.12	0.12	0.87	99.68	0.07	0.62	<d.l.	11.16	0.54		
	04SFAD03	1954-1801	C5	small pillow or tube	04SFAD03 CA01	50.48	1.435	14.01	9.52	1.91	0.189	7.32	11.43	2.64	0.14	0.10	0.70	99.87	0.01	0.73	<d.l.	11.24	0.54		
	04SFAD03	1954-1801	C6	crust of lava flow surface	04SFAD03 CA02	50.28	1.433	14.04	9.12	2.14	0.201	7.23	11.50	2.66	0.14	0.12	0.81	99.68	0.09	0.96	<d.l.	11.05	0.54		
	04SFAD04	1941-1925	C1	Fragments of autobrecciated lava	04SFAD04 CA01	51.32	1.809	15.91	8.23	3.35	0.221	5.00	8.74	3.27	0.43	0.21	3.02	99.51	0.65	2.50	<d.l.	11.24	0.44		
ERZ A	04SFAD05	2072-1955	C3	Fragments of autobrecciated lava	04SFAD05 CA02	48.54	2.382	12.54	10.48	3.72	0.229	4.81	8.92	3.06	0.36	0.23	4.73	99.90	0.66	4.55	<d.l.	13.83	0.38		
	04SFAD05	2072-1955	C2	Fragments of autobrecciated lava	04SFAD05 CA01	55.42	1.342	14.85	7.30	2.19	0.163	4.33	8.16	3.58	0.41	0.21	1.85	99.80	0.51	1.44	<d.l.	9.27	0.45		
	04SFAD05	2072-1955	C5	part of pillow lava	04SFAD05 CA02	54.63	1.290	14.60	7.27	2.05	0.173	4.22	7.99	3.57	0.40	0.21	3.01	99.42	0.84	2.53	<d.l.	9.11	0.45		
Jb-3																									
						51.36	1.393	17.17	7.63	3.31	0.174	5.13	9.67	2.76	0.76	0.28	0.29	99.93	0.21	0.60	<d.l.	10.61	0.46		

Area	Sampling No.	Depth (m)	No. of Individual Sample	Lithology	Sample No.	V	Ni	Th	U	Zr	Hf	Nb	Ta	Cs	Ba	Rb	Sr	Pb	Y						
						ppm	ppm	ppm	ppm	ppm	ppm	ppm	ppm	ppm	ppm	ppm	ppm	ppm	ppm	ppm					
ERZ A	04SFAD02	1954-1803	C3	vitric surface of basalt	04SFAD02 CA01	289	66.0	0.5	-0.1	93.2	3.5	2.6	0.15	1.8	22	<d.l.	86.6	1.7	27.6						
	04SFAD02	1954-1803	C5	Fragments of quenched basalt	04SFAD02 CA02	329	72.0	0.3	-0.1	104.0	3.1	2.8	0.17	3.2	23	0.4	97.0	0.8	36.2						
	04SFAD03	1954-1801	C5	small pillow or tube	04SFAD03 CA01	332	75.4	0.3	-0.1	107.0	3.0	2.7	0.14	3.2	20	0.2	92.1	0.6	35.3						
	04SFAD03	1954-1801	C6	crust of lava flow surface	04SFAD03 CA02	308	68.1	0.3	0.1	94.1	2.7	2.6	0.27	3.0	21	0.8	89.6	3.1	32.5						
	04SFAD04	1941-1925	C1	Fragments of autobrecciated lava	04SFAD04 CA01	299	54.6	0.7	0.4	184.6	4.9	4.7	0.43	1.9	72	<d.l.	112.5	3.8	42.2						
	04SFAD04	1941-1925	C3	part of pillow lava	04SFAD04 CA02	372	46.2	0.4	0.2	176.7	4.7	4.2	0.29	2.0	39	<d.l.	88.7	1.9	45.9						
ERZ A	04SFAD05	2072-1955	C2	Fragments of autobrecciated lava	04SFAD05 CA01	237	37.8	0.5	0.4	176.6	4.6	5.5	0.60	1.9	63	<d.l.	211.1	1.6	30.4						
	04SFAD05	2072-1955	C5	part of pillow lava	04SFAD05 CA02	201	35.4	0.5	0.3	157.7	4.0	5.2	0.49	2.3	55	<d.l.	185.4	1.3	25.6						
	Jb-3																								
						396	42.4	0.7	0.6	93.6	2.8	3.1	0.78	2.6	269	1.7	419.0	5.3	17.9						

Area	Sampling No.	Depth (m)	No. of Individual Sample	Lithology	Sample No.	La	Ce	Pr	Nd	Sm	Eu	Gd	Tb	Dy	Ho	Er	Tm	Yb	Lu						
						ppm	ppm	ppm	ppm	ppm	ppm	ppm	ppm	ppm	ppm	ppm	ppm	ppm	ppm	ppm					
ERZ A	04SFAD02	1954-1803	C3	vitric surface of basalt	04SFAD02 CA01	3.34	10.04	1.72	9.90	3.25	1.34	5.10	0.96	6.18	1.31	3.83	0.570	3.59	0.519						
	04SFAD02	1954-1803	C5	Fragments of quenched basalt	04SFAD02 CA02	3.43	10.36	1.75	10.43	3.55	1.39	5.28	1.00	6.55	1.37	4.10	0.609	3.82	0.549						
	04SFAD03	1954-1801	C5	small pillow or tube	04SFAD03 CA01	3.25	9.81	1.67	9.89	3.41	1.37	5.10	0.96	6.18	1.30	3.93	0.583	3.67	0.531						
	04SFAD03	1954-1801	C6	crust of lava flow surface	04SFAD03 CA02	3.18	9.69	1.69	9.98	3.36	1.38	5.12	0.97	6.32	1.34	4.00	0.603	3.79	0.530						
	04SFAD04	1941-1925	C1	Fragments of autobrecciated lava	04SFAD04 CA01	7.92	19.65	3.08	17.01	5.37	1.94	7.95	1.52	9.27	1.93	5.85	0.885	5.58	0.805						
	04SFAD04	1941-1925	C3	part of pillow lava	04SFAD04 CA02	6.25	17.65	2.96	16.56	5.41	2.02	8.32	1.59	9.91	2.07	6.18	0.926	5.93	0.862						
ERZ A	04SFAD05	2072-1955	C2	Fragments of autobrecciated lava	04SFAD05 CA01	9.81	23.05	3.32	16.50	4.87	1.69	6.57	1.24	7.53	1.59	4.74	0.714	4.50	0.649						
	04SFAD05	2072-1955	C5	part of pillow lava	04SFAD05 CA02	9.59	22.48	3.19	15.43	4.57	1.64	6.07	1.13	7.30	1.51	4.54	0.687	4.41	0.641						
	Jb-3																								
						9.21	22.22	3.28	16.13	4.25	1.38	4.93	0.83	4.76	0.95	2.73	0.401	2.52	0.371						

## 2-4 Interpretation of the Results

### 2-4-1 Norm calculations

The norm calculation was conducted using the analytical results and the results were shown on Table 4.

The samples collected at 04SFAD02 and 04SFAD03 are silica undersaturated rock with normative olivine and clinopyroxene, while samples collected from the at 04SFAD04 and 04SFAD005 are silica saturated rock with normative quartz. All the samples show high amount of normative pyroxenes and feldspar reaching more than 80%.

The analytical results were plotted to various diagrams for further discussion of classification of the rocks and tectonic setting of their origin.

### 2-4-2 Classification Diagrams( $\text{SiO}_2 - (\text{Na}_2\text{O} + \text{K}_2\text{O})$ , $\text{SiO}_2 - \text{K}_2\text{O}$ , AFM Diagrams)

The analytical results were normalizing to 100% by the total of ten major elements, they were plotted to  $\text{SiO}_2 - (\text{Na}_2\text{O} + \text{K}_2\text{O})$ ,  $\text{SiO}_2 - \text{K}_2\text{O}$ , AFM diagrams for discrimination of rock type.(Figures 1 to 3). According to the classification of Cox et al. (1979) all the samples collected at 04SFAD02 and 04SFAD03 and 04SFAD04CA02 are classified to basalt. While, 04SFAD04CA01 and the samples collected at 04SFAD05 are, respectively, classified into basaltic andesite and andesite (Figure 1). The all the samples are plotted in the area of low-K series volcanic rocks (Figure 2). Since the samples do not show a clear trend of differentiation, magmatic series can not be identified for these rocks (figure 3).

### 2-4-3 Tectonic Setting (Nb-Zr-Y, Ti-V Diagrams)

For considering the tectonic setting of origin of these rock analytical results were plotted on Nb-Zr-Y and Ti-V diagrams (Figures 4 and 5). Since these diagrams are only applicable for basaltic rocks, 04SFAD005 with andesitic composition was plotted only for reference. On the Nb-Zr-Y Diagrams which discriminate MORBs from within-plate basalt (Meschede, 1986, Figure 4), all the samples collected at 04SFAD02, 03 and 04 have similar composition to N-MORB and volcanic arc basalt. On the Ti-V diagram (Figure 5), all the samples collected at 04SFAD02 and 03 are plotted in the fields of MORB or BAB (Back arc basalt), while, samples of 04SFAD04 are plotted in the fields of MORB or BAB and continental flood basalt.

#### 2-4-4 Spidergram (normalized to N-MORB)

The analytical results are normalized to N-MORB and plotted to the spidergram (Figure 6a). For references typical basaltic rock from various tectonic settings were shown in Figure 6b using the data of Sun and McDonough (1989) and Shuutou and Gorai (1997). The samples of 04SFAD02 and 04SFAD03 show more or less similar concentrations and patterns to those of N-MORB except Ba. The concentrations and pattern are similar for samples of 04SFAD04 and 04SFAD05. Considering samples of 04SFAD05 are andesite, samples of 04SFAD04 with basaltic compositions are relatively enrich in LIL and HFS. The patterns of 04SFAD04 are similar to those of T-MORB (Transitional MORB), OIT (Oceanic Island Tholeiite) and WPT (Within Plate Tholeiite\_

#### 2-4-5 REE Diagram (normalized to N-MORB)

The analytical results are normalized to N-MORB of Sun and McDonough (1989) and REE diagram was drawn (Figure 7a). For references typical basaltic rock from various tectonic settings were shown in Figure 7b using the data of Sun and McDonough (1989) and Shuutou and Gorai (1997).

The samples collected at 04SFAD02 and 04SFAD03 show similar REE concentrations and patterns to those of N-MORB. The samples of 04SFAD05 have flat patterns of MREE (Middle Rare Earth, Sm~Ho) and HREE(Heavy Rare Earth Element, Er~Lu) and are very enriched in LREE (Light Rare Earth, La~Nd). The patters of 04SFAD04 samples are similar to that of T-MORB showing flat pattern with slightly declined LREE.

#### 2-5 Considerations

The all diagrams (Figures 4 to 7) show that the samples collected at 04SFAD02 and 04SFAD03 have similar chemical composition to that of MORB. The low K nature of these rocks conforms with the chemical nature of N-MORB. These samples are olivine basalt originated form the similar tectonic setting to the speeding axis of the mid-oceanic ridge.

The samples collected at 04SFAD04 are silica saturated basalt to basaltic andesite, and they show chemical characteristic different form N-MORB, rather similar to OIT, T-MORB, WPT (Figures 5 to 7). But their REE patterns do not show clear enrichment of LREE, which is characteristic feature of plume related rock such as E-MORB and OIT. The most probable basaltic type for these rocks is T-MORB slightly related to plume.

The silica saturated andesite of 04SFAD05 are unusual rock for oceanic



environment. Considering the low Ti despite of differentiated rock and enrichment of LREE, the possible tectonic setting for these rocks is newly born oceanic arc.

Table 4 Calculated Normal compositions

Sampling No.	Lithology	Sample No.	OI	Qz	Hy	Di	Or	Ab	An	Mt	Ap	Il	Total	Hy+Di	Or+Ab+An	Py+Fid
04SFAD02	vitric surface of basalt	04SFAD02 CA01	1.4	0.0	18.4	24.8	0.5	22.5	26.7	2.6	0.3	2.7	99.9	43.2	49.7	92.9
	fragments of quenched basalt	04SFAD02 CA02	1.1	0.0	18.7	24.7	0.7	22.5	26.3	2.8	0.3	2.8	99.9	43.4	49.6	93.0
04SFAD03	small pillow or tube	04SFAD03 CA01	0.9	0.0	18.9	24.8	0.8	22.5	26.2	2.8	0.2	2.7	99.9	43.7	49.5	93.2
	crust of lava flow surface	04SFAD03 CA02	0.5	0.0	18.4	25.1	0.8	22.8	26.3	3.1	0.3	2.8	99.9	43.4	49.9	93.3
04SFAD04	fragments of autobrecciated lava	04SFAD04 CA01	0.0	5.2	14.6	16.9	2.6	28.7	22.8	5.1	0.5	3.6	99.9	31.5	54.1	85.6
	part of pillow lava	04SFAD04 CA02	0.0	3.0	16.0	20.3	2.2	27.2	20.4	5.6	0.6	4.6	99.9	36.3	49.8	86.1
04SFAD05	fragments of autobrecciated lava	04SFAD05 CA01	0.0	8.9	14.2	13.3	2.5	30.9	23.7	3.2	0.5	2.6	99.9	27.6	57.1	84.7
	part of pillow lava	04SFAD05 CA02	0.0	8.7	14.5	13.4	2.5	31.3	23.5	3.1	0.5	2.5	99.9	27.8	57.3	85.1

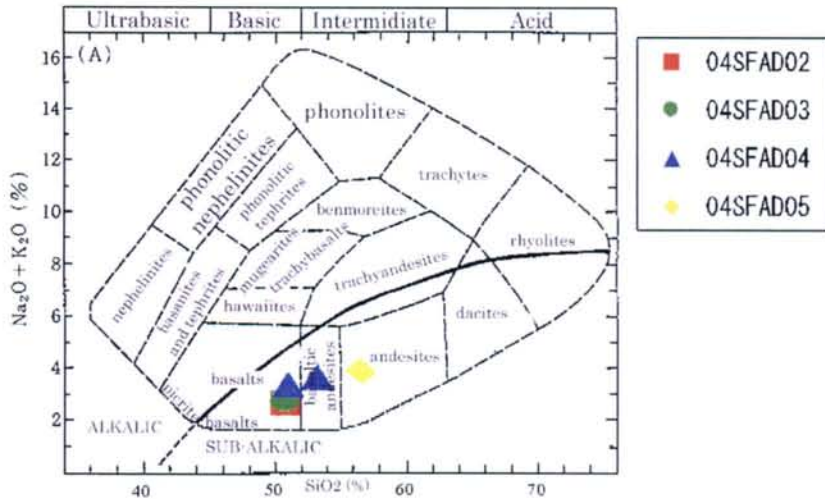


Fig1 Nomenclature of normal (i.e. non-potassic) igneous rocks after Cox et al.(1979). The dividing line between alkalic and sub-alkalic magma series is from Miyashiro (1978).

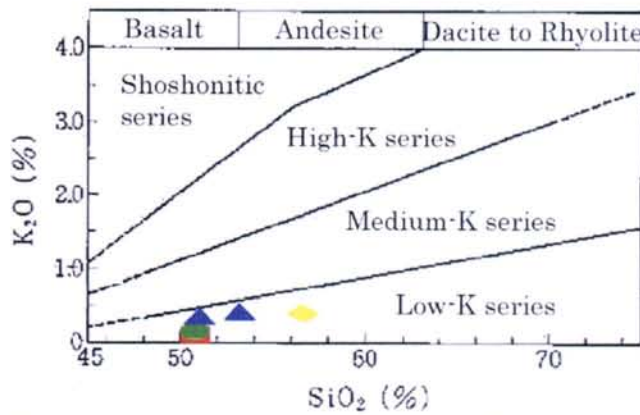


Fig2 Classification of alkalic and sub-alkalic volcanic rocks in terms of wt.% K2O versus wt.% SiO2 after Peccerillo and Taylor (1976).

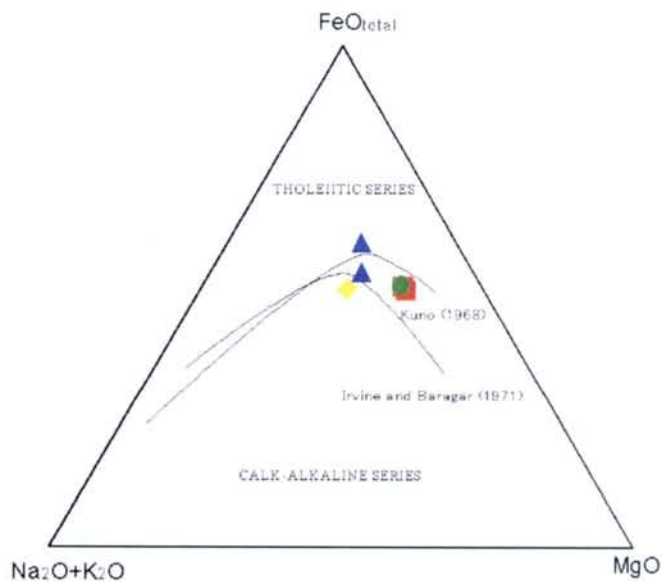


Fig3 AFM diagram showing typical tholeiitic and calc-alkaline differentiation trends.

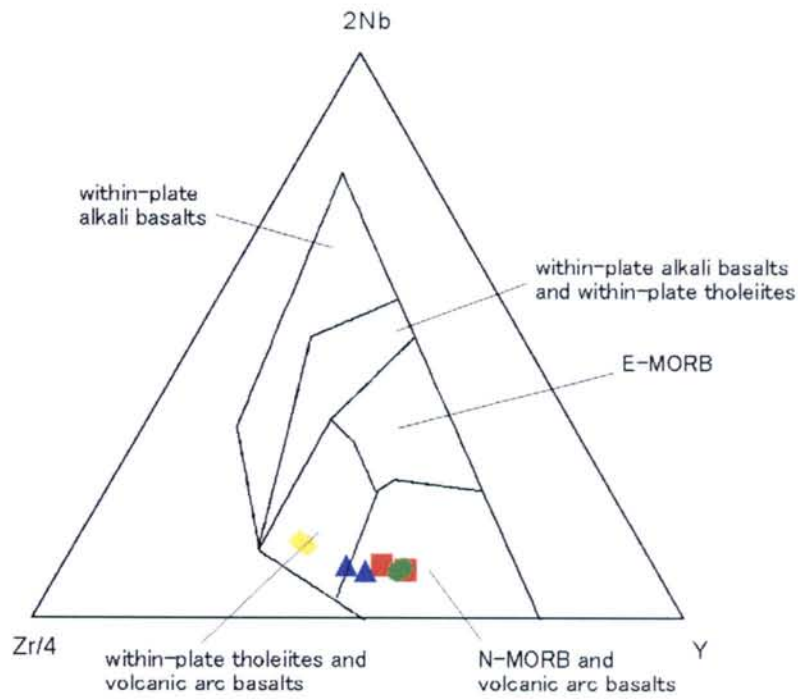


Fig4 2Nb-Zr/4-Y tectonomagmatic discrimination diagram for basaltic rocks (after Meschede 1986).

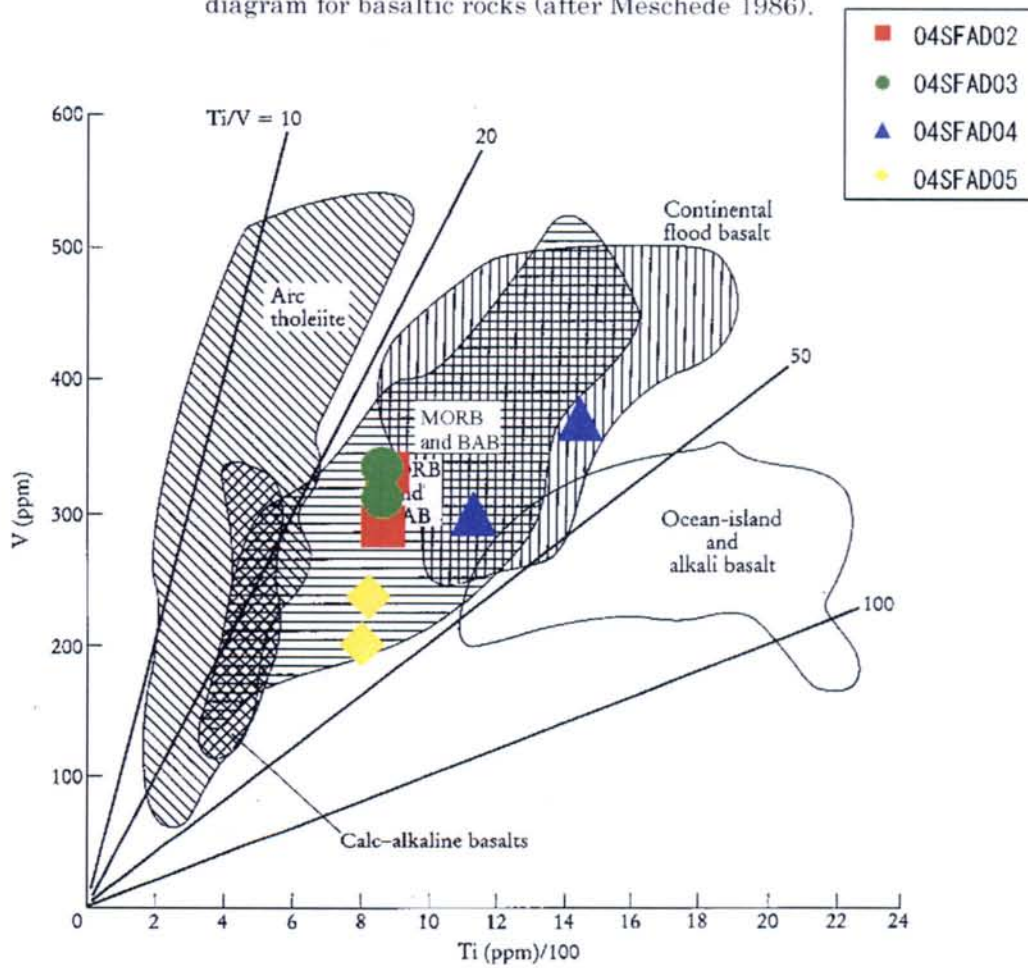


Fig5 Ti/1000 versus V (ppm) diagram, showing the discrimination of basaltic rocks after Shervais (1982).  
BAB : Back-Arc Basin basalt

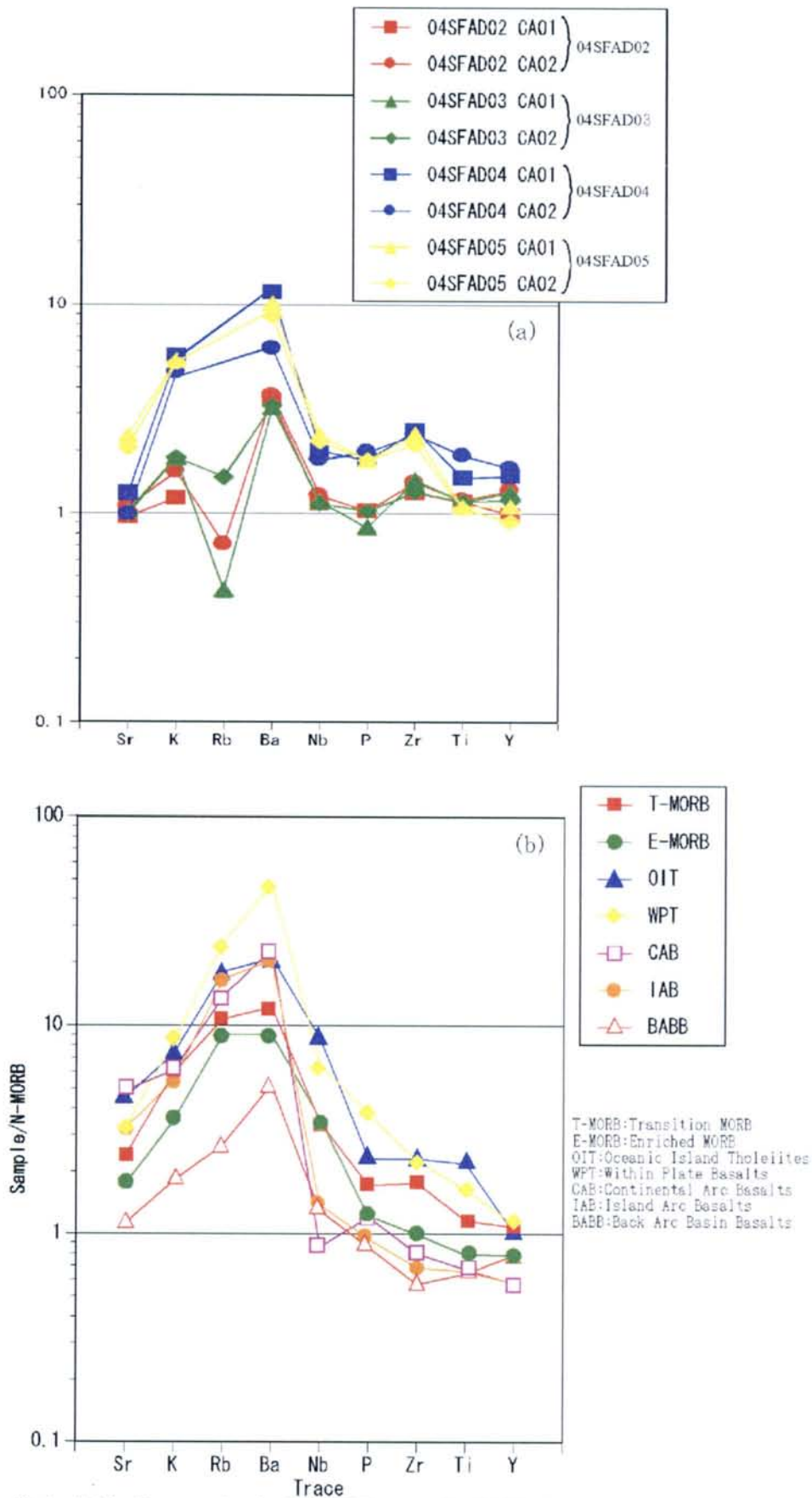


Fig6 Spiderdiagram for the N-MORB normalized LIL elements.

(a) Patterns for samples from the Fiji water

(b) Typical patterns for basalts

(N-MORB, E-MORB: Sun and McDonough, 1989

Others: Shuto and Gorai, 1997)

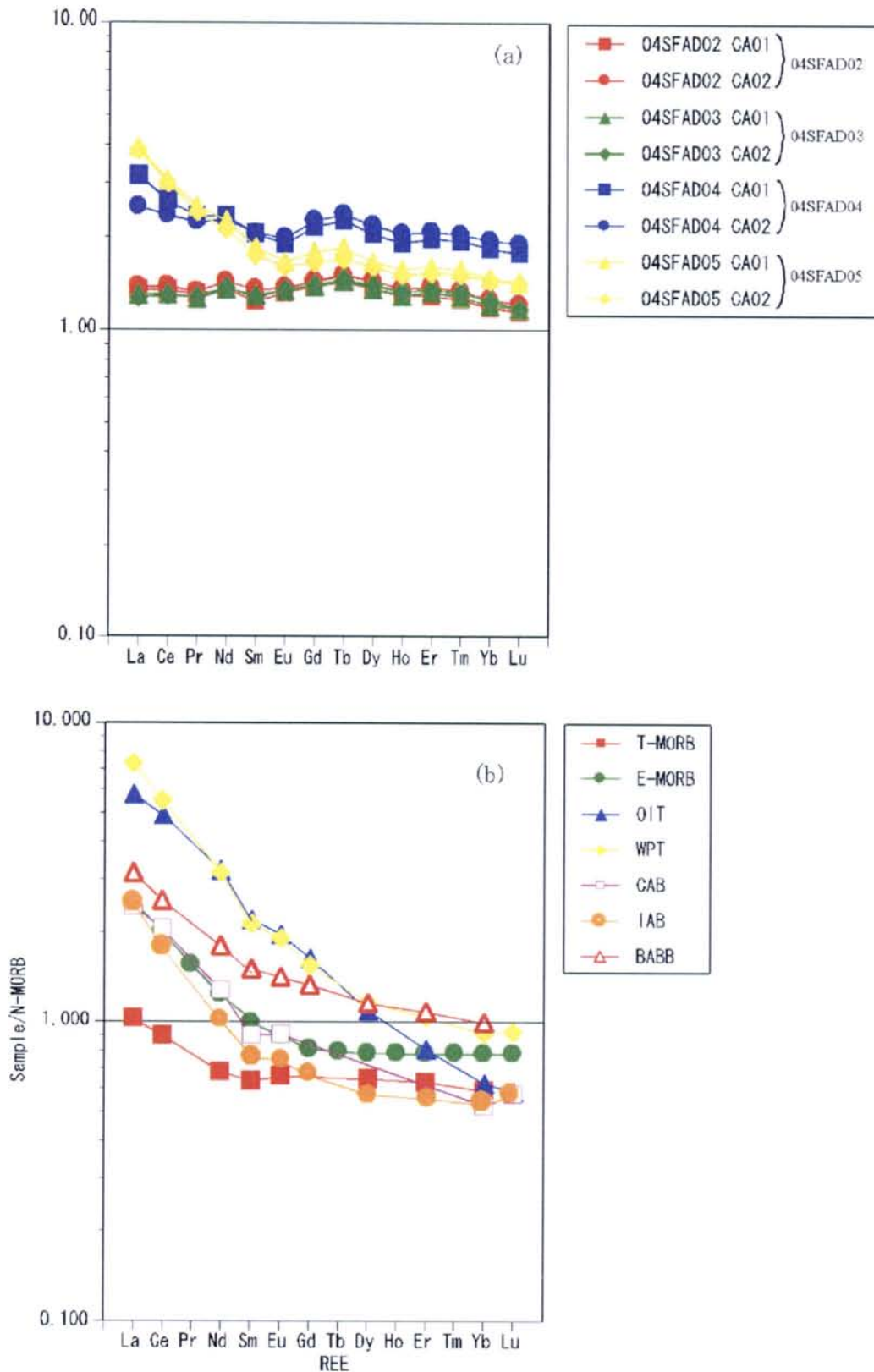


Fig7 N-MORB normalized REE patterns  
 (a) Patterns for samples from Fiji water  
 (b) Typical patterns for basalts  
 (N and E-MORB : Sun and McDonough, 1989  
 Others : Shuto and Gorai, 1997)

## 5-2 3. K-Ar Dating of Igneous Rocks

### 3-1 Samples

One sample was chosen from each sampling location and age determination by K-Ar was conducted for four samples from four AD sampling locations in the ERZ A (Table 1).

Table 1 Samples for K-Ar Age Determination

Sample No.	K (%)	Ar <sub>rad</sub> (nl/g)	<sup>40</sup> Ar <sub>air</sub> (%)	Age (Ma)
04SFAD02 KR01	0.088	0.504	81.6	144.3+6.8
04SFAD03 KR01	0.061	0.172	86.2	72.4+6.2
04SFAD04 KR01	0.273	0.032	96.5	3.1+1.6
04SFAD05 KR01	0.342	0.112	95.9	8.5+1.5
Reanalyses				
04SFAD02 KR01rep	0.089	0.513	81.9	145.0+4.6
04SFAD03 KR01rep	0.066	0.195	53.5	76.0+4.1

K : total K of sample

<sup>40</sup>Ar<sub>rad</sub>: radiogenetic <sup>40</sup>Ar of sample

<sup>40</sup>Ar<sub>air</sub>: present <sup>40</sup>Ar of air

### 3-2 Analytical Methods

The age determination by K-Ar method was conducted by Activation Laboratories Ltd, Canada. The analyses of six samples were carried out after desalination treatment and pulverization.

The K concentration was performed by ICP (Thermo Jarrell Ash, Enviro II) and the argon analysis was performed using the isotope dilution procedure on noble gas mass spectrometer.

For obtaining the age, following equation was used.

$$t = 1/(\lambda_{\beta} + \lambda_e) \ln((^{40}\text{Ar}_{\text{rad}} \cdot (\lambda_{\beta} + \lambda_e)) / (^{40}\text{K} \cdot \lambda_e) + 1)$$

where:

$\lambda_{\beta}$  : decay constant of <sup>40</sup>K to <sup>40</sup>Ca

$\lambda_e$  : decay constant of <sup>40</sup>K to <sup>40</sup>Ar

<sup>40</sup>Ar<sub>rad</sub> : radiogenetic <sup>40</sup>Ar of sample

<sup>40</sup>K : present <sup>40</sup>K of sample

### 3-3 Analytical Results

The results are shown in Table 7. Although four samples were collected from

similar geological environment, the samples 04SFAD02 KR01 and 04SFAD03 KR01 showed very unexpectedly old ages different from other two samples. The analyses of these two samples were conducted again, but similar ages to those of first analyses were obtained.

Table 2 Results of K-Ar dating

Sample No.	K(%)	Ar <sub>rad</sub> (nl/g)	<sup>40</sup> Ar <sub>air</sub> (%)	Age (Ma)
04SFAD02 KR01	0.088	0.504	81.6	144.3+6.8
04SFAD03 KR01	0.061	0.172	86.2	72.4+6.2
04SFAD04 KR01	0.273	0.032	96.5	3.1+1.6
04SFAD05 KR01	0.342	0.112	95.9	8.5+1.5
Reanalyses				
04SFAD02 KR01rep	0.089	0.513	81.9	145.0+4.6
04SFAD03 KR01rep	0.066	0.195	53.5	76.0+4.1

K: total K of sample

<sup>40</sup>Ar<sub>rad</sub>: radiogenetic <sup>40</sup>Ar of sample

<sup>40</sup>Ar<sub>air</sub>: present <sup>40</sup>Ar of air

### 3-4 Considerations

A wide range of ages, 3.1+/-1.6Ma to 144.3+/-6.8Ma, was obtained from K-Ar dating of 4 basaltic lava samples. The reasons for this are probably because analyzed samples are pillow lavas consisting of inhomogeneous materials including vitric parts and obtained ages were affected by excess <sup>40</sup>Ar.

2



## Appendix 5

### Laboratory Works 5 – 3

1. X-ray Diffraction of Alteration Products
2. Ore Analysis
3. Chemistry of sediments
4. Microfossils in sediments

### 5-3 1. X-Ray Diffraction of Alteration Products

#### 1-1 Samples for X-Ray Diffraction Analyses

The X-ray diffraction analyses were conducted for altered rock and sediments for characterizing alteration and identifying some of the minerals (Table1).

Table 1 Sample List of X-ray Diffraction Analysis

Area	Sample No.	Depth (m)	Sampling Depth / No. of Individual Sample	Description	Sample No.
Central Hill	04SFFPG01	1,971		white vein penetrating serpentinite	04SFFPG01 XRD01
	04SFFPG03	1,968		black altered part of serpentinite	04SFFPG03 XRD01
				black precipitates on surface	04SFFPG03 XRD02
				detrital sandy clay	04SFFPG03 XRD03
				pale bluish gray clay	04SFFPG03 XRD04
				dark gray pebble in pale bluish gray clay	04SFFPG03 XRD05
				reddish brown precipitate	04SFFPG03 XRD06
				white acicular crystals in druses occur in bluish gray clayey part	04SFFPG03 XRD07
	04SFMC11	1,946	0.00	black and white clayey precipitates	04SFMC11 XRD01
			0.15-0.18	foraminifera sand	04SFMC11 XRD02
ERZ A	04SFAD02	1,956→1,803		greenish altered part of lava flow	04SFAD02 XRD01
	04SFAD02	1,956→1,803	C10	altered basalt	04SFAD02C10 XRD01
					04SFAD02C10 XRD02
					04SFAD02C10 XRD03
			C11	altered basalt	04SFAD02C11 XRD04
			04SFAD02C11 XRD05		

#### 1-2 Analytical Methods

The X-ray diffraction analyses were conducted by Prof. K. Watanabe at Kyushu University using x-ray diffractometer of Rigaku RINT2100. Powder patterns were obtained by Cu K $\alpha$  radiation scanning 2-70 degree at scan speed of 2 degree per a minute. The examined samples includes nonoriented and oriented powders and treated powders by HCl and ethylene glycol.

### 1-3 Results of Analyses

The results of X-ray diffraction analyses are given on Table 2. The relative abundance of minerals is shown as quartz index. The quartz index was proportionally obtained, as given below, considering the diffraction intensity of 101 plain of standard quartz as 100%

Quartz Index of Mineral A = (Intensity of the maximum peak of Mineral A/Intensity of 101 plain of standard quartz) x 100

### 1-4 Considerations

#### 1-4-1 Central Hill

##### (1) 04SFFPG01

-XRD01 (white vein penetrating serpentinite): Aragonite peak was obtained and the vein penetrating serpentinite consists of aragonite.

##### (2) 04SFFPG03

-XRD01 (black altered part of serpentinite): Serpentine, calcite, aragonite, chromite and brucite were identified. These minerals are alteration products of the ultramafic rocks.

-XRD02 (black precipitates on surface): Peaks of quartz, albite and calcite were obtained. The reason for black color is not unknown, but they are mineral assemblages of altered felsic materials.

-XRD03 (detrital sandy clay): Tremolite, chlorite, serpentine and talc were identified. These are mineral assemblages of altered ultramafic rocks.

-XRD04 (pale bluish gray clay): Albite, tremolite, serpentine, calcite and aragonite were identified and this sample is considered to be alteration materials of ultramafic rocks.

-XRD05 (dark gray pebble in pale bluish gray clay): Serpentine, calcite, aragonite, chromite and pyrite were identified. These minerals suggest that the pebble is altered ultramafic rock..

-XRD06 (reddish brown precipitates): The mineral assemblages found by X-ray diffraction, such as serpentine, calcite, aragonite and chromite suggest this precipitates to be alteration materials of ultramafic rock.

-XRD07 (white acicular crystals in druses occur in bluish gray clayey part): Serpentine and aragonite were identified. The white acicular crystals are aragonite.

##### (3) 04SFMC11

-XRD01 (black and white clayey precipitates): Calcite, magnesite or rhodochrosite, aragonite and Todorokite were identified. The black precipitates are probably reflecting todorokite and the white precipitates consist of mixture of various carbonates.

-XRD02 (foraminifera sand): serpentine, calcite, magnesite or rhodochrosite, aragonite and todorokite were identified. The foraminifera sand consists of calcareous fragments of foraminifera, and alteration materials of ultramafic rocks are included in them.

#### 1-4-2 ERZ A

##### (1) 04SFAD02

-XRD01 (greenish altered part of lava flow): Smectite was identified and green color reflects the smectite alteration of lava flow.

##### (2) 04SFAD02C10

-C10XRD01 (altered basalt): Smectite was identified. The basalt is altered to smectite.

-C10XRD02 (altered basalt): Peaks of smectite, serpentine and todorokite are obtained. This sample seems to be altered olivine basalt with coating of manganese oxides.

-C10XRD03 (altered basalt): Same as C10XRD02, smectite, serpentine and todorokite were identified. This sample seems to be altered olivine basalt with coating of manganese oxides.

##### (3) 04SFAD02C11

-C11XRD04 (altered basalt): Peaks of smectite and todorokite were obtained. This sample seems to be altered basalt with coating of manganese oxides.

-C11XRD05 (altered basalt): Same as C11XRD05, peaks of smectite and todorokite were obtained. This sample seems to be altered basalt with coating of manganese oxides

Table 2 Results of X-ray Diffraction Analysis

Area	Sampling No.	Sampling Depth / No. of Individual Sample	Description	Sample No.	Silicate							Carbonates				Other minerals				Remarks							
					Silica Minerals	Feldspar	Others	Clay minerals				Tremolite	Calcite	Calcite(*)	Aragonite	Chromite	Pyrite	Todorokite	Brucite								
								Quartz	Albite	Talc	Smectite										Chlorite	Serpentine	Talc				
Central Hill	04SFFPG01		white vein penetrating serpentinite	04SFFPG01 XRD01																							
			black altered part of serpentinite	04SFFPG03 XRD01																							
			black precipitates on surface	04SFFPG03 XRD02																							
			derrial sandy clay	04SFFPG03 XRD03					2.8																		
			pale bluish gray clay	04SFFPG03 XRD04																							
			dark gray pebble in pale bluish gray clay	04SFFPG03 XRD05																							
			reddish brown precipitates	04SFFPG03 XRD06																							
			white acicular crystals in cluses occur in bluish gray clayey part	04SFFPG03 XRD07																							
			black and white clayey precipitates	04SFMFC11 XRD01																							
			foraminifera sand	04SFMFC11 XRD02																							
		greenish altered part of lava flow	04SFAD02 XRD01																								
ERZ A				04SFAD02 XRD01																							
		C10	altered basalt	04SFAD02 XRD02																							
				04SFAD02 XRD03																							
				04SFAD02 XRD04																							
			altered basalt	04SFAD02 XRD05																							

numbers are given in % calcite(\*) : calcite, manganous or magnesian tr : identified only by oriented poeders unknown peak d=2.81

## 5-3 2. Chemical Analyses of Altered Rocks

### 2-1 Samples

Altered and discolored rocks of the Central Hill were selected for chemical analyses to characterize the alteration and possible mineralization of the area (Table 1).

**Table 1 Sample List of Chemical Analysis**

Area	Sample No.	Depth (m)	Lithology	Sample No.
Central Hill	04SFFPG01	1,971	black serpentinite	04SFFPG01 CR01
			yellowish brown serpentinite	04SFFPG01 CR02
	04SFFPG03	1,968	white alteration vein and serpentinite	04SFFPG03 CR01
			conglomerate with reddish brown precipitates	04SFFPG03 CR02
			bluish gray clayey materials	04SFFPG03 CR03

### 2-2 Analytical Methods and Elements

A total of 54 elements, including platinum group elements (PGE), Au, Ag and transition metallic elements, were analyzed. Analyzed elements, analytical methods, detection limits are given in Table 2. The chemical analyses were mainly conducted at ALS Chemex, Canada, except PGE and Au, which were analyzed in Genalysis Laboratory Service Pty. Ltd, Australia. Before the chemical analyses desalination of the samples were conducted by supersonic washer using the deionized water for twenty four hours, repeating three times.

### 2-3 Analytical Results

The analytical results are shown on Table 3.

**Table 2 Analyzed Elements and Analytical Method**

Analyzed Elements (lower limit-upper limit)	Analytical Method
Ag (1-1,000ppm), Cu (0.01-50%), Co (0.001-50%), Ni (0.01-50%), Pb (0.01-30%), Zn (0.01-30%), Fe (0.01-30%), As (0.01-30%), Cd (1ppm-10%), Sb (0.01-100%)	Atomic Absorption Spectrometer
Pt, Pd, Ru, Rh, Os, Ir, Au (1ppb- ), Ag (5-3,500ppm)	Fire Assay+ICP-MS
S (0.01-50%)	Infrared Absorption Analysis
Hg (0.01-100ppm)	Cold Vapor-AAS
Fe (0.01-100%), Zn (0.01-100%)	Titration
Ti (0.005-10%), P (10-10,000ppm), Mn (5-10,000ppm), Cr, V (1-10,000ppm)	ICP-AES
Ba (10-10,000ppm), W (0.1-10,000ppm), Mo (0.05-10,000ppm), Be, Sb (0.05-1000ppm), Bi (0.01-10,000ppm)	ICP-AES and ICP-MS
Se (1-1,000ppm), La, Zr (0.5-500ppm), Li, Sn, Th (0.2-500ppm), Hf, Nb, Rb, U, Y (0.1-500ppm), Cs, Ga, Ge, Te (0.05-500ppm), Ta (0.05-100ppm), Tl (0.02-500ppm), Ce (0.01-500ppm), In (0.005-500ppm), Re (0.002-50ppm)	ICP-MS
H <sub>2</sub> O <sup>+</sup> (0.01-100%), C (0.01-50%)	LECO
H <sub>2</sub> O <sup>-</sup> (0.01-100%)	After drying at 105 deg.C gravitationally determined
LOI (0.01-100%)	After fusing at 1000 deg.C gravitationally determined

## **2-4 Statistical Analyses**

### **2-4-1 Univariate Analysis**

For statistical Treatment analytical values less than detection limit are treated as a half value of detection limit. The statistical values, such as maximum, minimum, average, standard deviation and coefficient of variation, are given on Table 4. No significant differences of concentration between sampling locations 04SFFPG01 and 04SFFPG03 was observed except Mn which shows slightly higher average value in 04SFFPG03 than in 04SFFPG01.

### **2-4-2 Multi-variant Analyses**

Correlation coefficients were calculated and non correlation test was carried out (Tables 5 and 6). As the results, HFS (Ti, Al, Mn, P, Th,  $\delta$ , Zr, Hf, Nb, Ta) and REE (La, Ce, Pr, Nd, Sm, Eu, Gd, Tb, Dy, Ho, Er, Tm, Yb, Lu) show good correlation. The HFS and REE are known to show similar behavior during episodes of magmatic and hydrothermal activities. The correlation coefficients obtained are reflecting this point. Si, Ti, Mn, V, Cr and Fe are included in serpentine and oxides included in serpentine, while Ca, P and C are included in carbonates.

### **2-4-3 REE Normalized Patterns**

The REE of the analyzed samples were normalized to primordial mantle (McDonough et al., 1991) for serpentinite samples ((04SFFPG01 CR01, CR02 and 04SFFPG03 CR01) and to North American Standard Shale (Gromet et al., 1984) for conglomerate and clay sample. The REE normalized patterns are shown in Figures 1 and 2.

Two serpentinite show similar REE pattern, showing high LREE, right side declining pattern. The concentrations of REE are less compared to the primordial mantle except La. Although these samples were strongly altered, chemical characteristics of low REE concentration less than primordial mantle and higher LREE are similar to those of forearc serpentine.

Conglomerate and clay samples shows lower concentrations of REE compared to the North American Standard Shale. Although the concentrations are low, 04SFFPG03CR02 show flat pattern of REE, showing similar concentration ratio of REE compared to those of the North American Standard Shale.





Table 4 Statistical Values

Statistical Values	SiO <sub>2</sub>	TiO <sub>2</sub>	Al <sub>2</sub> O <sub>3</sub>	FeO	Fe <sub>2</sub> O <sub>3</sub>	MnO	MgO	CaO	Na <sub>2</sub> O	K <sub>2</sub> O	P <sub>2</sub> O <sub>5</sub>	H <sub>2</sub> O <sup>+</sup>	H <sub>2</sub> O <sup>-</sup>	C	LOI	Ti	V
	%	%	%	%	%	%	%	%	%	%	%	%	%	%	%	%	ppm
No. of Samples	5	5	5	5	5	5	5	5	5	5	5	5	5	5	5	5	5
Maximum	34.30	0.06	0.70	3.55	8.20	0.50	35.40	11.25	0.09	0.03	0.10	12.05	0.52	2.48	18.55	0.031	76
Minimum	31.10	0.01	0.28	0.51	3.54	0.04	31.20	3.75	0.02	0.01	0.01	9.94	0.20	0.82	15.35	0.00	24
Average	32.54	0.02	0.40	2.04	5.33	0.15	33.04	8.53	0.07	0.02	0.04	10.67	0.35	1.88	16.65	0.01	48
Standard Deviation	1.38	0.02	0.17	1.22	2.01	0.20	1.56	3.09	0.03	0.01	0.04	0.96	0.12	0.68	1.34	0.01	19
Coefficient of Variation	0.043	1.118	0.439	0.596	0.376	1.313	0.047	0.362	0.409	0.354	0.991	0.090	0.350	0.360	0.080	1.55	0.392

Statistical Values	Cr	Mn	Fe	Co	Ni	Cu	Zn	Th	U	Zr	Hf	Nb	Ta	Cs	Ba	Rb	Sr
	ppm	ppm	%	%	%	%	%	ppm	ppm	ppm	ppm	ppm	ppm	ppm	ppm	ppm	ppm
No. of Samples	5	5	5	5	5	5	5	5	5	5	5	5	5	5	5	5	5
Maximum	4300	3830	6.60	0.016	1535	0.01	0.02	0.3	1.9	24.9	0.50	2.3	0.050	0.060	40	0.7	2070
Minimum	3810	460	4.72	0.006	1015	0.01	0.01	0.1	0.5	2.9	0.05	0.1	0.025	0.025	5	0.2	674
Average	4024	1222	5.48	0.010	1238	0.01	0.01	0.1	0.9	7.9	0.15	0.6	0.030	0.032	14	0.4	1551
Standard Deviation	223	1461	0.77	0.004	193	0.00	0.01	0.1	0.6	9.5	0.20	1.0	0.011	0.016	15	0.2	585
Coefficient of Variation	0.056	1.196	0.140	0.422	0.156	0.391	0.391	0.639	0.633	1.214	1.312	1.660	0.373	0.489	1.057	0.458	0.378

Statistical Values	La	Ce	Pr	Nd	Sm	Eu	Gd	Tb	Dy	Ho	Er	Tm	Yb	Lu	Y	Rh
	ppm	ppm	ppm	ppm	ppm	ppm	ppm	ppm	ppm	ppm	ppm	ppm	ppm	ppm	ppm	ppb
No. of Samples	5	5	5	5	5	5	5	5	5	5	5	5	5	5	5	5
Maximum	5.3	10.6	0.90	3.90	0.90	0.20	0.90	0.10	1.00	0.20	0.70	0.10	0.60	0.10	5.1	2.0
Minimum	0.3	0.3	0.05	0.25	0.05	0.05	0.05	0.05	0.05	0.05	0.05	0.05	0.05	0.05	0.05	0.6
Average	1.6	2.7	0.23	1.05	0.24	0.09	0.26	0.06	0.26	0.08	0.19	0.06	0.18	0.06	1.9	1.0
Standard Deviation	2.1	4.5	0.38	1.60	0.37	0.07	0.36	0.02	0.41	0.07	0.29	0.02	0.24	0.02	1.8	0.6
Coefficient of Variation	1.327	1.682	1.631	1.524	1.541	0.724	1.396	0.373	1.594	0.839	1.505	0.373	1.312	0.373	0.972	0.612

Statistical Values	Pt	Pd	Li	Be	Mo	W	Re	Ga	In	Tl	Ge	Sn	P	Bi	S	Te
	ppb	ppb	ppm	ppm	ppm	ppm	ppm	ppm	ppm	ppm	ppm	ppm	ppm	ppm	%	ppm
No. of Samples	5	5	5	5	5	5	5	5	5	5	5	5	5	5	5	5
Maximum	24	6	2.3	0.180	7.97	1.0	0.003	1.68	0.012	1.22	0.13	0.3	390	0.210	2.85	0.90
Minimum	7	3	0.5	0.025	1.00	0.1	0.001	0.55	0.003	0.01	0.11	0.1	90	0.005	0.03	0.05
Average	13	4	1.7	0.056	3.38	0.3	0.001	0.94	0.004	0.36	0.12	0.2	188	0.077	1.07	0.23
Standard Deviation	7	1	0.7	0.069	2.97	0.4	0.001	0.44	0.004	0.50	0.01	0.1	118	0.090	1.31	0.38
Coefficient of Variation	0.501	0.261	0.431	1.238	0.880	1.282	0.639	0.462	0.966	1.406	0.071	0.465	0.628	1.168	1.225	1.667

Table 5 Correlation Coefficient

Table with 18 columns for element pairs (SiO2, TiO2, Al2O3, FeO, MnO, MgO, CaO, Na2O, K2O, P2O5, H2O, H2O2, CO2, LOI, Ti, V, Cr, Mn, Fe, Co, Ni, Cu, Zn, Th, U, Zr, Hf, Nb, Ta, Cs, Ba, Rb, Sr) and rows for various elements (SiO2, TiO2, Al2O3, FeO, MnO, MgO, CaO, Na2O, K2O, P2O5, H2O, H2O2, CO2, LOI, Ti, V, Cr, Mn, Fe, Co, Ni, Cu, Zn, Th, U, Zr, Hf, Nb, Ta, Cs, Ba, Rb, Sr).

\*Correlation coefficient < 0

Table 5 Correlation Coefficient

simple correlation coefficient	La	Ce	Pr	Nd	Sm	Eu	Gd	Tb	Dy	Hb	Er	Tm	Yb	Lu	Y	Rh	Pt	Fd	Li	Be	Mo	W	Re	Cs	In	Tl	Ge	Sn	P	Bi	S	Te				
La	1.0000																																			
Ce	0.9941	1.0000																																		
Pr	0.9912	0.9950	1.0000																																	
Nd	0.9883	0.9900	0.9955	1.0000																																
Sm	0.9851	0.9835	0.9803	0.9765	1.0000																															
Eu	0.9809	0.9854	0.9802	0.9888	0.9927	0.9925	1.0000																													
Gd	0.9826	0.9859	0.9865	0.9858	0.9877	0.9852	0.9857	1.0000																												
Tb	0.9821	0.9850	0.9855	0.9870	0.9881	0.9853	0.9822	0.9852	1.0000																											
Dy	0.9820	0.9849	0.9853	0.9868	0.9878	0.9851	0.9827	0.9856	0.9871	1.0000																										
Er	0.9823	0.9863	0.9868	0.9882	0.9893	0.9865	0.9849	0.9871	0.9885	0.9871	1.0000																									
Tm	0.9817	0.9860	0.9865	0.9879	0.9890	0.9862	0.9846	0.9868	0.9882	0.9894	0.9871	1.0000																								
Yb	0.9826	0.9869	0.9874	0.9888	0.9899	0.9871	0.9855	0.9877	0.9891	0.9904	0.9882	0.9869	1.0000																							
Lu	0.9822	0.9865	0.9870	0.9884	0.9895	0.9867	0.9851	0.9873	0.9887	0.9900	0.9878	0.9865	0.9852	1.0000																						
Rh	0.8512	0.8259	0.8277	0.8344	0.8414	0.8381	0.8272	0.8311	0.8354	0.8401	0.8371	0.8354	0.8372	0.8376	0.8411	1.0000																				
Pt	0.8501	0.8267	0.8284	0.8351	0.8421	0.8388	0.8279	0.8322	0.8365	0.8412	0.8382	0.8365	0.8383	0.8387	0.8422	0.8411	1.0000																			
Fd	0.9202	0.7415	0.7245	0.7269	0.8019	0.8102	0.7908	0.8198	0.8307	0.8195	0.7659	0.8138	0.8316	0.8215	0.8248	0.8215	0.8215	0.8215	0.8215	0.8215	0.8215	0.8215	0.8215	0.8215	0.8215	0.8215	0.8215	0.8215	0.8215	0.8215	0.8215	0.8215	0.8215	0.8215		
Li	0.9202	0.2445	-0.2794	-0.2116	-0.3460	-0.2454	-0.2509	-0.2158	-0.2509	-0.2158	-0.2509	-0.2158	-0.2509	-0.2158	-0.2509	-0.2158	-0.2509	-0.2158	-0.2509	-0.2158	-0.2509	-0.2158	-0.2509	-0.2158	-0.2509	-0.2158	-0.2509	-0.2158	-0.2509	-0.2158	-0.2509	-0.2158	-0.2509			
Be	0.9202	0.2445	-0.2794	-0.2116	-0.3460	-0.2454	-0.2509	-0.2158	-0.2509	-0.2158	-0.2509	-0.2158	-0.2509	-0.2158	-0.2509	-0.2158	-0.2509	-0.2158	-0.2509	-0.2158	-0.2509	-0.2158	-0.2509	-0.2158	-0.2509	-0.2158	-0.2509	-0.2158	-0.2509	-0.2158	-0.2509	-0.2158	-0.2509			
Mo	0.9202	0.2445	-0.2794	-0.2116	-0.3460	-0.2454	-0.2509	-0.2158	-0.2509	-0.2158	-0.2509	-0.2158	-0.2509	-0.2158	-0.2509	-0.2158	-0.2509	-0.2158	-0.2509	-0.2158	-0.2509	-0.2158	-0.2509	-0.2158	-0.2509	-0.2158	-0.2509	-0.2158	-0.2509	-0.2158	-0.2509	-0.2158	-0.2509			
W	0.9202	0.2445	-0.2794	-0.2116	-0.3460	-0.2454	-0.2509	-0.2158	-0.2509	-0.2158	-0.2509	-0.2158	-0.2509	-0.2158	-0.2509	-0.2158	-0.2509	-0.2158	-0.2509	-0.2158	-0.2509	-0.2158	-0.2509	-0.2158	-0.2509	-0.2158	-0.2509	-0.2158	-0.2509	-0.2158	-0.2509	-0.2158	-0.2509			
Re	0.9202	0.2445	-0.2794	-0.2116	-0.3460	-0.2454	-0.2509	-0.2158	-0.2509	-0.2158	-0.2509	-0.2158	-0.2509	-0.2158	-0.2509	-0.2158	-0.2509	-0.2158	-0.2509	-0.2158	-0.2509	-0.2158	-0.2509	-0.2158	-0.2509	-0.2158	-0.2509	-0.2158	-0.2509	-0.2158	-0.2509	-0.2158	-0.2509			
Cs	0.9202	0.2445	-0.2794	-0.2116	-0.3460	-0.2454	-0.2509	-0.2158	-0.2509	-0.2158	-0.2509	-0.2158	-0.2509	-0.2158	-0.2509	-0.2158	-0.2509	-0.2158	-0.2509	-0.2158	-0.2509	-0.2158	-0.2509	-0.2158	-0.2509	-0.2158	-0.2509	-0.2158	-0.2509	-0.2158	-0.2509	-0.2158	-0.2509			
In	0.9202	0.2445	-0.2794	-0.2116	-0.3460	-0.2454	-0.2509	-0.2158	-0.2509	-0.2158	-0.2509	-0.2158	-0.2509	-0.2158	-0.2509	-0.2158	-0.2509	-0.2158	-0.2509	-0.2158	-0.2509	-0.2158	-0.2509	-0.2158	-0.2509	-0.2158	-0.2509	-0.2158	-0.2509	-0.2158	-0.2509	-0.2158	-0.2509			
Tl	0.9202	0.2445	-0.2794	-0.2116	-0.3460	-0.2454	-0.2509	-0.2158	-0.2509	-0.2158	-0.2509	-0.2158	-0.2509	-0.2158	-0.2509	-0.2158	-0.2509	-0.2158	-0.2509	-0.2158	-0.2509	-0.2158	-0.2509	-0.2158	-0.2509	-0.2158	-0.2509	-0.2158	-0.2509	-0.2158	-0.2509	-0.2158	-0.2509			
Ge	0.9202	0.2445	-0.2794	-0.2116	-0.3460	-0.2454	-0.2509	-0.2158	-0.2509	-0.2158	-0.2509	-0.2158	-0.2509	-0.2158	-0.2509	-0.2158	-0.2509	-0.2158	-0.2509	-0.2158	-0.2509	-0.2158	-0.2509	-0.2158	-0.2509	-0.2158	-0.2509	-0.2158	-0.2509	-0.2158	-0.2509	-0.2158	-0.2509			
Sn	0.9202	0.2445	-0.2794	-0.2116	-0.3460	-0.2454	-0.2509	-0.2158	-0.2509	-0.2158	-0.2509	-0.2158	-0.2509	-0.2158	-0.2509	-0.2158	-0.2509	-0.2158	-0.2509	-0.2158	-0.2509	-0.2158	-0.2509	-0.2158	-0.2509	-0.2158	-0.2509	-0.2158	-0.2509	-0.2158	-0.2509	-0.2158	-0.2509			
P	0.9202	0.2445	-0.2794	-0.2116	-0.3460	-0.2454	-0.2509	-0.2158	-0.2509	-0.2158	-0.2509	-0.2158	-0.2509	-0.2158	-0.2509	-0.2158	-0.2509	-0.2158	-0.2509	-0.2158	-0.2509	-0.2158	-0.2509	-0.2158	-0.2509	-0.2158	-0.2509	-0.2158	-0.2509	-0.2158	-0.2509	-0.2158	-0.2509			
Bi	0.9202	0.2445	-0.2794	-0.2116	-0.3460	-0.2454	-0.2509	-0.2158	-0.2509	-0.2158	-0.2509	-0.2158	-0.2509	-0.2158	-0.2509	-0.2158	-0.2509	-0.2158	-0.2509	-0.2158	-0.2509	-0.2158	-0.2509	-0.2158	-0.2509	-0.2158	-0.2509	-0.2158	-0.2509	-0.2158	-0.2509	-0.2158	-0.2509			
S	0.9202	0.2445	-0.2794	-0.2116	-0.3460	-0.2454	-0.2509	-0.2158	-0.2509	-0.2158	-0.2509	-0.2158	-0.2509	-0.2158	-0.2509	-0.2158	-0.2509	-0.2158	-0.2509	-0.2158	-0.2509	-0.2158	-0.2509	-0.2158	-0.2509	-0.2158	-0.2509	-0.2158	-0.2509	-0.2158	-0.2509	-0.2158	-0.2509			
Te	0.9202	0.2445	-0.2794	-0.2116	-0.3460	-0.2454	-0.2509	-0.2158	-0.2509	-0.2158	-0.2509	-0.2158	-0.2509	-0.2158	-0.2509	-0.2158	-0.2509	-0.2158	-0.2509	-0.2158	-0.2509	-0.2158	-0.2509	-0.2158	-0.2509	-0.2158	-0.2509	-0.2158	-0.2509	-0.2158	-0.2509	-0.2158	-0.2509			

\* correlation coefficient = 0





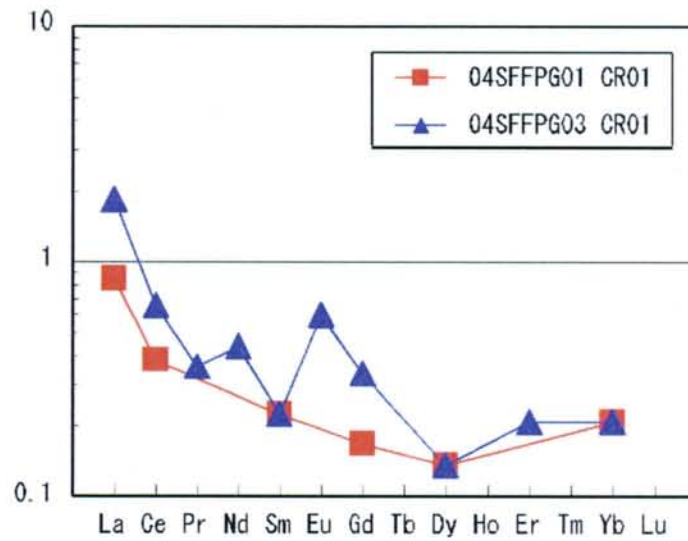


Fig 1. REE abundance patterns, normalized to chondritic abundances, for serpentinites from Fiji water.

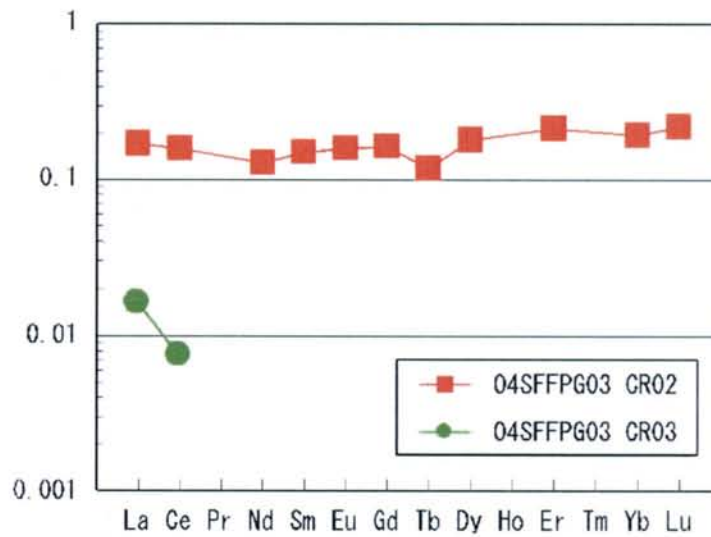


Fig 2. REE abundance patterns, normalized to the North American Standard Shale's abundances, for conglomerate and clay from Fiji Water.

### 5-3 3. Chemistry Sediments

#### 3-1 Samples

The chemical analyses were conducted for the unconsolidated sediments (foraminifera sand) collected in the Central Hill (Table 1).

**Table 1 Sample List of Unconsolidated Sediments**

Area	Sampling No.	Depth (m)	Sampling Depth (m)	Geology	Sample No.
Central Hill	04SFMC11	1,946	0.10-0.15	foraminifera Sand	04SFMC11 CS01
			0.15-0.18	foraminifera Sand	04SFMC11 CS02

#### 3-2 Analytical Method

A total of 34 elements, such as major elements, platinum group elements, gold, silver and trace elements, were analyzed. Analyzed elements, analytical methods, detection limits are given in Table 2. The chemical analyses were mainly conducted at ALS Chemex, Canada, except platinum group elements and Au, which were analyzed in Genalysis Laboratory Service Pty. Ltd, Australia. Before the chemical analyses desalination of the samples were conducted by supersonic washer using the deionized water for twenty for hours, repeating three times.

**Table 2 Analyzed Elements and Analytical Method**

Analyzed Elements (lower limit-upper limit)	Analytical Method
Al, Ca, Fe (0.01%-25%), Mg (0.01-15%), K, Na (0.01-10%), Ti (0.005-10%), P (10-10,000ppm), Mn (5-10,000ppm), Zn (2-10,000ppm), Cr, V (1-10,000ppm)	ICP-AES
Ba (10-10,000ppm), Pb (0.5-10,000ppm), As, Cu, Ni, Sr (0.2-10,000ppm), Co, W (0.1-10,000ppm), Mo (0.05-10,000ppm), Be, Sb (0.05-1,000ppm), Bi (0.01-10,000ppm), Cd (0.02-500ppm), Ag (0.01-100ppm)	ICP-AES and ICP-Mass
Mn (0.01-50%)*	Atomic Absorption Spectrometer
Rh (1ppb)	NiS collection Fire Assay + ICP-MS
Pt, Pd, Ru, Os, Ir (2ppb)	
Au (5ppb)	
Hg (0.01-100ppm)	Cold Vapor-Atomic Absorption Spectrometer
* only 04SFMC11 CS02	



### 3-3 Results

The analytical results of unconsolidated sediments are shown on Table 3

### 3-4. Considerations

Corresponding to the results of X-ray diffraction analysis of 04SFMC11 with calcite and aragonite peaks, both samples CS01 and CS02 show high Ca contents reflecting abundant fragments of foraminifera included in the sediments. The both samples show high content of Mn suggesting the inclusions of manganese oxides particles or precipitates in the foraminifera sand. This coincides with the occurrence of todorokite identified by X-ray diffraction analyses in 04SFMC11 XRD02. Higher Mn associated by higher Ni and Cu in 04SFMC11 CS02 than in 04SFMC11 CS01 suggest that the former includes more particles or precipitates of manganese oxides than the latter.

Among platinum group elements (PGE) only Pt was detected, however, it is within the error range. Consequently, no significant PGE was contained in the samples.

Table 3 Analytical Results of Unconsolidated Sediments.

Area	Depth (m)	Sample No.	Al	Ca	Fe	Mg	K	Na	Ti	P	Mn	Zn	Cr	V	Ba	Pb	As	Cu	Ni	
			%	%	%	%	%	ppm	ppm	ppm	ppm	ppm	ppm	ppm	ppm	ppm	ppm	ppm	ppm	ppm
Central Hill	1,946	04SFMC11 CS01	0.66	35.7	0.42	0.77	0.05	0.23	0.042	300	1730	25	49	12	50	6.7	12	27.8	16.5	
		04SFMC11 CS02	0.61	35.3	0.43	0.94	0.08	0.25	0.042	310	26200*	51	82	16	70	4.1	<5	36.2	60.3	
Area	Depth (m)	Sample No.	Sr	Co	W	Mo	Be	Sb	Bi	Cd	Ag	Hg	Os	Ir	Ru	Rh	Pt	Pd	Au	
			ppm	ppm	ppm	ppm	ppm	ppm	ppm	ppm	ppm	ppm	ppm	ppm	ppb	ppb	ppb	ppb	ppb	ppb
Central Hill	1,946	04SFMC11 CS01	1465	2.5	0.2	0.34	0.09	0.28	<0.01	0.39	0.12	0.02	<d.l.	<d.l.	<d.l.	<d.l.	<d.l.	2	<d.l.	<d.l.
		04SFMC11 CS02	1435	4.9	1	5.32	<0.05	1.52	<0.01	0.99	0.13	0.02	<d.l.	<d.l.	<d.l.	<d.l.	<d.l.	2	<d.l.	<d.l.

### 5-3 4. Microfossils in Sediments

#### 4-1 Sample for Fossil Identifications

Fossil identification was conducted for unconsolidated sediments collated in the Central Hill by MC (Table 1).

Table 1 Sample for Fossil Identification

Area	Sampling No.	Depth (m)	Location of sample (m)	Lithology	Sample No.
Central Hill	04SFMC11	1,946	0.10-0.18	foraminifera sand	04SFMC11 FS01

#### 4-2 Analytical Methods and Results

For determination of sedimentation age of the unconsolidated sediments, inspections of planktonic foraminifer, ichthyolith and radiolaria were conducted. The analytical methods and results are given below on each fossil type basis. The fossil inspections were conducted by following researchers as shown on Table 2.

Table 2 Inspector of Fossils

Fossil Type	Inspector	Institutions
planktonic foraminifer	Motoyoshi Oda	Professor, Tohoku University
ichthyolith	Kaoru Oogane	PhD student, Tohoku University
radiolaria	Noritaka Suzuki	Assistant Professor, Tohoku University

##### 4-2-1 Planktonic Foraminifer

###### (1) Analytical Method

To a beaker, 30g of unconsolidated sediments was taken and each individuals fossil was separated rinsing by 3% hydrogen peroxide. After filtering by 63-micrometer mesh, dried by oven. Planktonic foraminifers of more than 150 micrometer across were identified under microscope magnifying 40 times.

###### (2) Results

The planktonic foraminifers shown on Table 3 were identified from the unconsolidated sediments.

As the identified planktonic foraminifers, such as *Globigerinoides rubber*, *G. sacculifer*, *G. conglobatus*, *Globorotalia*, *Sphaeroidinella dehiscens* and *Pulleniatina*

*obliquiloculata*, belong to tropical to sub-tropical group (Be, 1977), the biostratigraphic standard of the low latitude (Blow, 1969; Berggren et al., 1985, 1995) can be applied for geological age determination.

Table 3 Results of Planktonic Foraminifer Identification

Species	Abundance
<i>G. bulloides</i> d'Orbigny	R
<i>Globigerinella aequilateralis</i> (Brady)	R
<i>G. calida</i> Parker	R
<i>Globigerinita glutinata</i> (Egger)	R
<i>G. conglobatus</i> (Brady)	F
<i>G. ruber</i> (d'Orbigny)Pink	C
<i>G. ruber</i> (d'Orbigny)White	R
<i>G. sacculifer</i> (Brady)	C
<i>Globorotalia crassaformis</i> (Galloway and Wissl	R
<i>G. menardii</i> (Parker, Jones and Brady)	F
<i>G. truncatulinoides</i> (d'Orbigny)	R
<i>G. tumida</i> (Brady)	R
<i>Neogloboquadrina dutertrei</i> (d'Orbigny)	R
<i>O. universa</i> (d'Orbigny)	R
<i>Pulleniatina obliquiloculata</i> (Parker and Jones )	R
<i>Sphaeroidinella dehiscens</i> (Parker and Jones)	R

R: Rare,F: Few,C: Common

Following biostratigraphic events and geological ages were used for estimating the geological age of this area.

- 1) extinction of pink individual of *Globigerinoides ruber* : 0.12Ma
- 2) appearance of *Globigerinella calida calida* : 0.3 Ma
- 3) extinction of *Globorotalia tosaensis* :0.6 Ma
- 4) appearance of *Globorotalia truncatulinoides* :2.0Ma

From the evidences that *Globorotalia truncatulinoides* occurs and *Globorotalia tosaensis* was not found and that *Globigerinella calida calida* and pink individuals of *Globigerinoides rubber* occur, the geological age of this sample is estimated to be late Pleistocene.

#### 4-2-2 Ichthyolith

##### (1) Analytical Method

The ichthyolith fossils were collected by following manner. At first, sediments sample was rinsed by 3% hydrogen peroxide to separate individual fossils. After rinsing by water, calcareous materials such as foraminifer were removed by 5% acetic acid. Then, it was filtered by 63-micrometer mash and the remnants on the mesh were collected for picking up ichthyolith individuals by microscope. The collected Ichthyolith fossils were sealed in the slide glass and the identification of Ichthyolith was conducted using the biological microscope.

Estimation of geological age was done based on Doyle and Riedel (1985), which was most recently established biostratigraphy of Ichthyolith.

## (2) Results

The sub-types of Ichthyolith related to determining geological age are listed in Table 4 and photographs of typical Ichthyolith found in the sample are shown in Figure 1.

Table 4 Sub-Types of Ichthyolith

Sub-Type	Age
<i>Flexed triangle 120-128</i>	0.0Ma-32.4Ma
<i>Rectangular saw-toothed</i>	0.0Ma-32.4Ma
<i>Triangle with high inline apex</i>	0.0Ma-32.4Ma
<i>Triangle with base angle</i>	0.0Ma-32.4Ma
<i>Small triangle with long striation</i>	0.0Ma-32.4Ma

All of the sub-types of Ichthyolith included in the sample, such as *Rectangular saw-toothed*, *Triangle with high inline apex*, *Triangle with base angle* and *Small triangle with long striation*, belong to the sub-types that appeared after 32.4 Ma. Consequently, geological age of 0.0Ma to 32.4Ma was estimated for the sample. This corresponds to the evidence that the sub-type of Ichthyolith that disappeared before 32.4Ma were not found in the sample.

## 4-2-3 Radiolaria

### (1) Analytical Method

For concentrating siliceous microfossils, calcareous part was removed by conc-hydrochloric acid, and hydrogen peroxide and surface-active agent, calgon, were used for dissolving organic materials and clay minerals, respectively. Then, the sample was filtered by 38-micrometer mesh and the remnants were investigated by microscope. The microscopic observation resulted in finding no fragment of radiolaria. The sample

was further examined by suspended materials separation method without using chemicals for concentration of siliceous microfossils. The result of microscopic observation of the remnants obtained by this method revealed only one fragment with similar appearance to radiolaria.

### (3) Results

Since only one fragment with similar appearance to radiolaria was found in the sample, it was impossible to estimate geological age and paleoenvironment from the sample. It is known that species of radiolaria are rare in the area close to the sampling location (177-25.847E, 16-5.692S) located at the boundary zone of nonproductive zone of radiolaria in the South Pacific (eg. Lombardi and Boden 1985). The evidence of no radiolaria found in the sample suggests that the area of the sampling location is probably situated inside the nonproductive zone of radiolaria.

### 4-3 Conclusions

The results of the fossil identification are given in Table 5.

Table 5 Results of Fossil Identification

Area	Sampling No.	Sampling Depth (m)	Sample No.	Ichthyolith	Planktonic Foraminifer	Radiolaria
Central Hill	04SFMC11	0.10-0.18	04SFMC11 FS01	0.0-32.4Ma	Late Pleistocene	very poor occurrence

The fossil identification suggests that the sedimentation of the sample started in late Pleistocene in the nonproductive zone of radiolaria.

Plate

Photomicrographs of Microfossils

A. Ichthyolith • Planktonic Foraminifer

(Scale bar is 100  $\mu$  m)

fig. 1 *Flexed triangle 120-128*

Photo ID P1260217

fig. 2 *Rectangular saw-toothed*

Photo ID P1260221

fig. 3 *Triangle with high inline apex*

Photo ID P1260227

fig. 4 *Triangle with base angle*

Photo ID P1260235

fig. 5 *Small triangle with long striation*

Photo ID P1260253

fig. 6 *Globorotalia truncatulinoides*

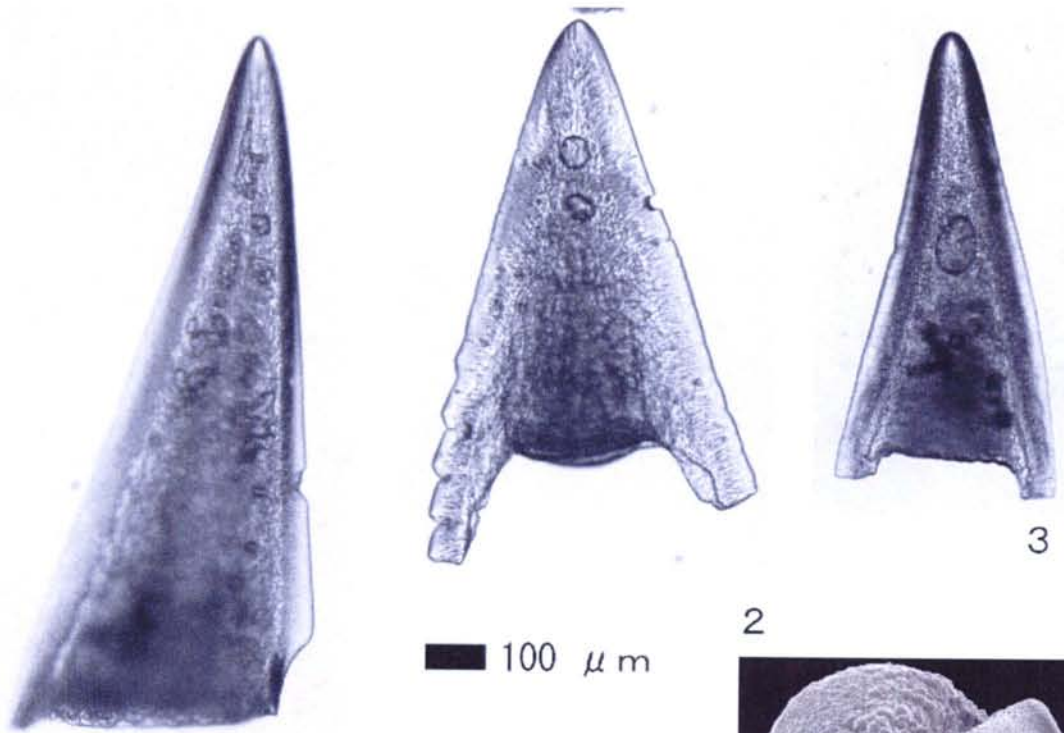
Photo ID image004

fig. 7 *Globigerinella calida calida*

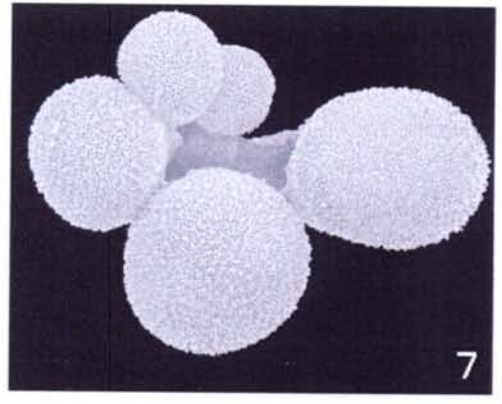
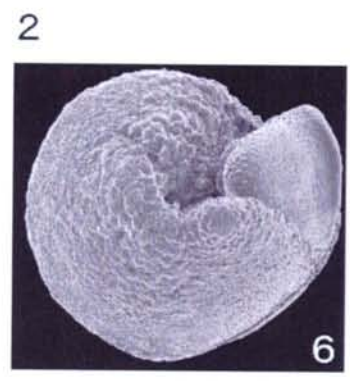
Photo ID cal.1-u070



Plate 1



100  $\mu$ m



Appendix 6  
Environmental Survey

# Appendix 6 Environmental Survey

## Contents

### 1. Objectives

### 2. Sampling Area

### 3. Materials and Methods

#### 3-1 Study Subjects

#### 3-2 Survey Methods

### 4. Results

#### 4-1 Survey Station

#### 4-2 Water Quality and Bacterioplankton

##### 4-2-1 Water Quality

##### 4-2-2 Bacterioplankton

##### 4-2-3 Summary

#### 4-3 Bottom Sediment and Benthic Organism

##### 4-3-1 Bottom Sediment

##### 4-3-2 Benthic Organisms

##### 4-3-3 Summary

### 5. Conclusion

## **1. Objectives**

The environmental survey was carried out in designated areas as a baseline study to evaluate the magnitude of mining impacts on deep-sea environment. The survey was done to understand: 1) the condition of water quality and the distribution of microorganisms in the water (referred hereafter as the, "water quality/bacterioplankton survey"), and 2) the condition of bottom-sediment properties and the composition of benthic organisms (referred hereafter as the, "bottom sediment and benthic organism survey").

## **2. Sampling Area**

The areas selected for sampling are shown in Figures 2-1 and 2-2. Two sampling sites were used for the research: Central Hill of 16°00'S, 177°20'W and ERZA of 16°20'S, 177°20'W. Central Hill is a seamount situated at a water depth of 2,500 m and ERZA has a fairly level topography located at a water depth of 2,000 m.

## **3. Materials and Methods**

### **3-1 Study Subjects**

#### **3-1-1 Water Quality/Bacterioplankton Survey**

- (1) Water quality: water temperature and salinity
- (2) Microorganisms: bacterioplankton

#### **3-1-2 Bottom Sediment and Benthic Organism Survey**

The following surveys were conducted using a multiple corer (MC). Prior to sampling, a video observation was carried out to select sites with large accumulation of sediments. Samples for macrobenthic organisms were obtained from mineral samples, which were collected using a power glove (FPG) or arm dredge (AD).

- (1) Bottom-sediment properties: water content, calcium carbonate, total organic carbon, total nitrogen, total sulfide, and specific gravity.
- (2) Benthic organisms: sedimentary bacteria, meiobenthos, and macrobenthos.

### **3-2 Survey Methods**

#### **3-2-1 Observation, Sampling, and Processing of Samples**

- (1) Water quality/Bacterioplankton Survey

Water temperature and salinity were measured using a CTD (SEA-BIRD: MODEL 9 PLUS) attached to a rosette sampler (RO). Measurements of these parameters were carried out from the surface layer to 10 m depth above the sea floor. The instrument was dropped at 0.5 m/sec, and measurement interval was set as once per second.

Samples for bacterioplankton was taken using a Niskin water sampler (with a capacity of 1.7 liters) attached to an RO, from 12 layers (10 m, 50 m, 75 m, 100 m, 125 m, 150 m, 175 m, 200 m, 250 m, 300 m, 500 m, and 1,000 m) from the sea floor. Samples were treated accordingly as described in Table 3-2-1.

(2) Bottom sediment and benthic organism survey

Sediment samples for the “bottom sediment and benthic organism survey” (excluding macrobenthos) were taken using MC. To minimize the possibility of hitting gravels, thus reducing the incidence of core obstruction, the number of cores was reduced from eight to four. Samples were sliced every 1 cm from the surface to 8 cm depth of the sediment. Samples were then treated accordingly as described in Table 3-2-1.

**Table 3 - 2 - 1 Sample processing and preservations**

Subject	Sample processing and preservations
Bacterioplankton	Fixed by glutaraldehyde (1 % v/v) and stained by DAPI (1µg/ml), filtered by nuclepore filter (0.2µm), mounted on a slide glass; frozen
Water Content, Specific Gravity, CaCO <sub>3</sub> , TOC, T – N	Frozen
T – S	Fixed by Zinc ammine; refrigerated
Sedimentary Bacteria	Fixed by glutaraldehyde (1 % v/v); refrigerated
Meiobenthos	Fixed by neutralized formalin (10 % v/v) and stained by Rose Bengal; refrigerated
Macrobenthos	Fixed by neutralized formalin (10 % v/v)

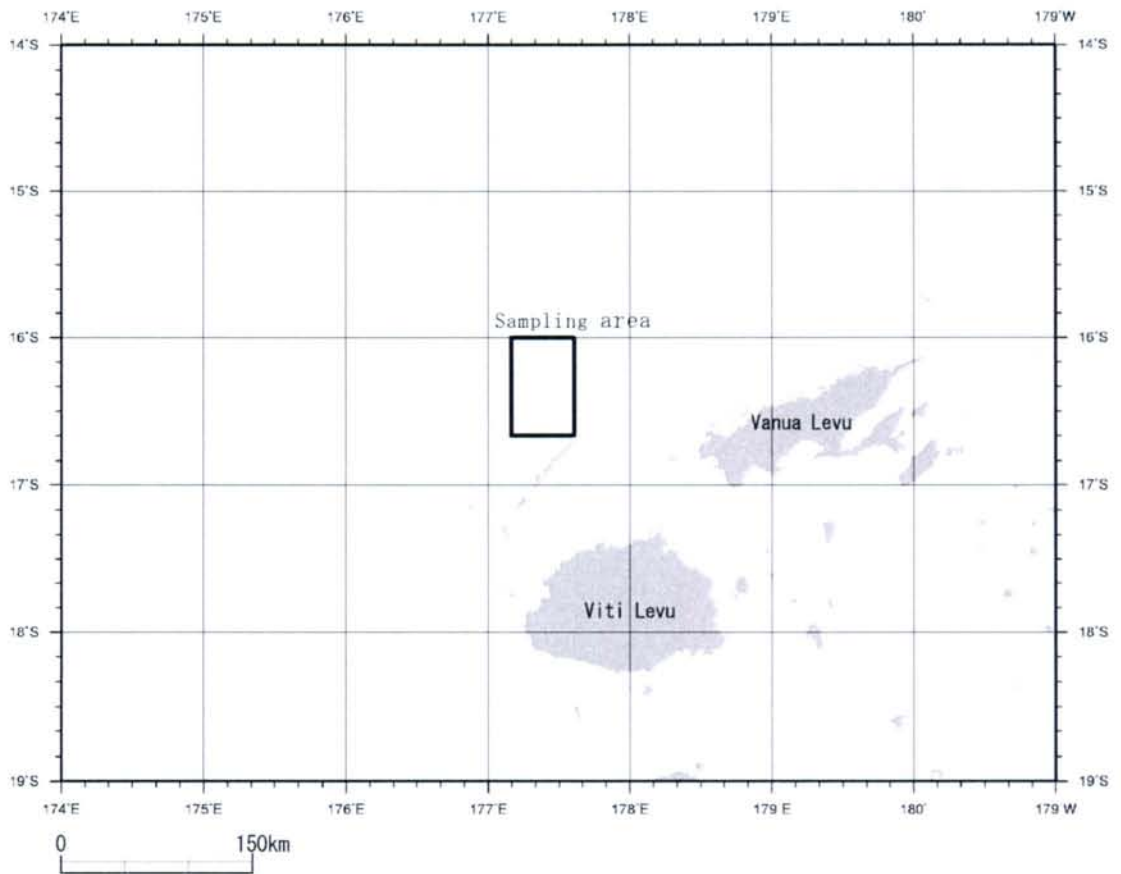
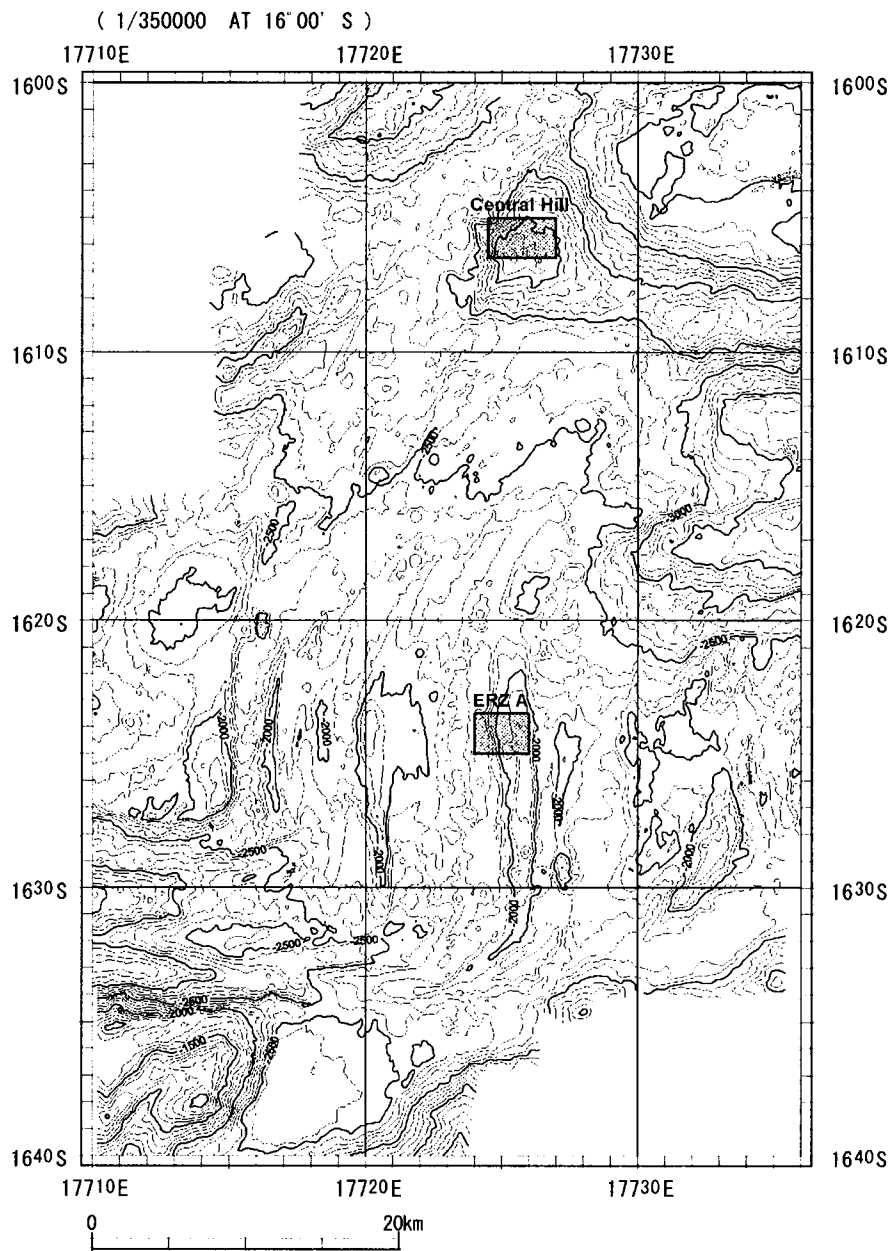


Figure 2 - 1 Sampling area (1)



**Figure 2 - 2 Sampling area (2)**



### 3-2-2 Analysis of Samples

#### (1) Water quality/Bacterioplankton survey

##### 1) Bacterioplankton

Bacterioplankton on the nuclepore filters were counted using an epifluorescence microscope. Abundance was expressed as the total number of bacteria per unit volume of seawater.

#### (2) Bottom sediment and benthic organism survey

##### 1) Water Content

The wet sample was weighed, desiccated in a dryer (60°C) until a constant weight was obtained, and then weighed again.

##### 2) Calcium Carbonate

After the water content of the sample had been measured, the total carbon in the dry sample was measured with a CHN analyzer (MT-5 made by Yanaco). The amount of inorganic carbon was obtained as the difference between the total carbon and the organic carbon. Then, assuming that the inorganic carbon existed in the form of calcium carbonate, the quantity of this compound was calculated from the element ratio.

##### 3) Total Organic Carbon (TOC) and Total Nitrogen (T-N)

After the water content had been determined, the dry sample was measured with a CHN analyzer (MT-5 made by Yanaco) to find the total amounts of carbon and nitrogen. The sample was treated with 4-N hydrochloric acid and reaction was allowed to occur for about one hour to remove the inorganic carbon. The sample was then desiccated again and measured with the CHN analyzer in the same way to find the organic carbon content.

##### 4) Total Sulfide (T-S)

The fixed sample was filtered with a glass fiber filter (GF/F) and the residue was distilled under an acidic condition using sulfuric acid. The extract obtained through filtration was re-fixed in zinc acetate dihydrate solution (10%) and was titrated using a sodium thiosulfate pentahydrate solution (1/100 N). The data obtained through titration was standardized into a unit of dry weight using water contents measured previously, so as to determine the total sulfide.

##### 5) Specific Gravity

The sample was dried to a constant weight at 110°C and then milled in an agate mortar. This was measured into a specific gravity bottle to about 10 grams. Distilled water was added into the sample and was heated in a water bath chamber for 4 hours.

It was left untouched for a whole day after which, the temperature and weight of the specific gravity bottle were measured.

#### 6) Sedimentary Bacteria

The bacteria bonding to the bottom sediment particles were exfoliated using an ultrasonic treatment into a settled solution, and then a fractional quantitation of the supernatant liquid was taken. This was stained with a DAPI (with a final concentration of 1  $\mu$ g/ml) and filtered. The trapped sediment was mounted on a glass slide and the number of bacteria was counted using an epifluorescence microscope. The total amount of bacteria per unit quantity of dry sediment was calculated from the dry weight of the bottom sediment material, which had been measured separately.

#### 7) Meiobentos

The sample stained with rose bengal was sieved by of 32  $\mu$ m and 300  $\mu$ m mesh sieve. Organisms were identified and counted under a microscope.

#### 8) Macrobenthos

The sample was sieved using a 300  $\mu$ m mesh sieve to separate out the sand and mud. Organisms that were trapped in the sieve were identified and counted.

## 4. Results

### 4-1 Survey Stations

The water quality/bacterioplankton survey were carried out at two stations (Central Hill: 04SFRO06, ERZA: 04SFRO07) while the sediment properties and benthic organism (excluding macrobenthic) surveys were carried out at three stations in Central Hill (04SFMC09, 04SFMC10, 04SFMC11). The macrobenthos survey as carried out at four stations in the Central Hill (04SFFPG01, 04SFFPG02, 04SFFPG03, 04SFAD07) and at one station in the ERZA (04SFAD05), (Figures 4-1-1 and 4-1-2).

### 4-2 Water Quality and Bacterioplankton

#### 4-2-1 Water Quality

##### (1) Water temperature

The water temperature ranged from 28.6°C (at the surface layer) to 2.3°C (at 1,914 m depth) at 04SFRO06 and from 28.8°C (at the surface layer) to 2.2°C (at 1,923 m depth) at 04SFRO07. The vertical distribution of the water temperature of the whole water column did not significantly differ between the two stations. The temperature decreased remarkably from the surface to 600 m depth and minimal change was observed from 600 m to 2,000 m depth (Figure 4-2-1).

## (2) Salinity

At 04SFRO06, the salinity increased at around 30 m, showing a maximum value (about 35.2 PSU) at around 170 m. However, it decreased remarkably until around 700 m depth (about 33.8 PSU) and then increased gradually again until about 2,000 m (Figure 4-2-1). At 04SFRO07, the salinity increased at around 20 m, reaching a maximum of 35.9 PSU at around 130 m, and decreased remarkably to 34.4 PSU around 700 m, and then increased gradually again until around 2,000 m (Figure 4-2-1).

### 4-2-2 Bacterioplankton

At 04SFRO06, the abundances of bacterioplankton showed a maximum abundance of  $1.86 \times 10^4$  cells / ml at 914 m depth, but decreased to  $1.04 \times 10^4$  cells / ml at 1,616 m depth. In the deeper layer, abundances showed an oscillating pattern, showing a maximum ( $1.33 \times 10^4$  cells/ml) at 1,716 m and a minimum ( $9.55 \times 10^3$  cells/ml) at 1,787 m depth (Figure 4-2-2 and Appendix 1).

At 04SFRO07, the abundances were  $1.40 \times 10^4$  cells / ml at 932 m depth and observed a maximum ( $1.53 \times 10^4$  cells / ml) at 1,681 m depth. In the deeper than this layer, it decreased to  $1.02 \times 10^4$  cells / ml at 1,806 m depth (Figure 4-2-2 and Appendix 1).

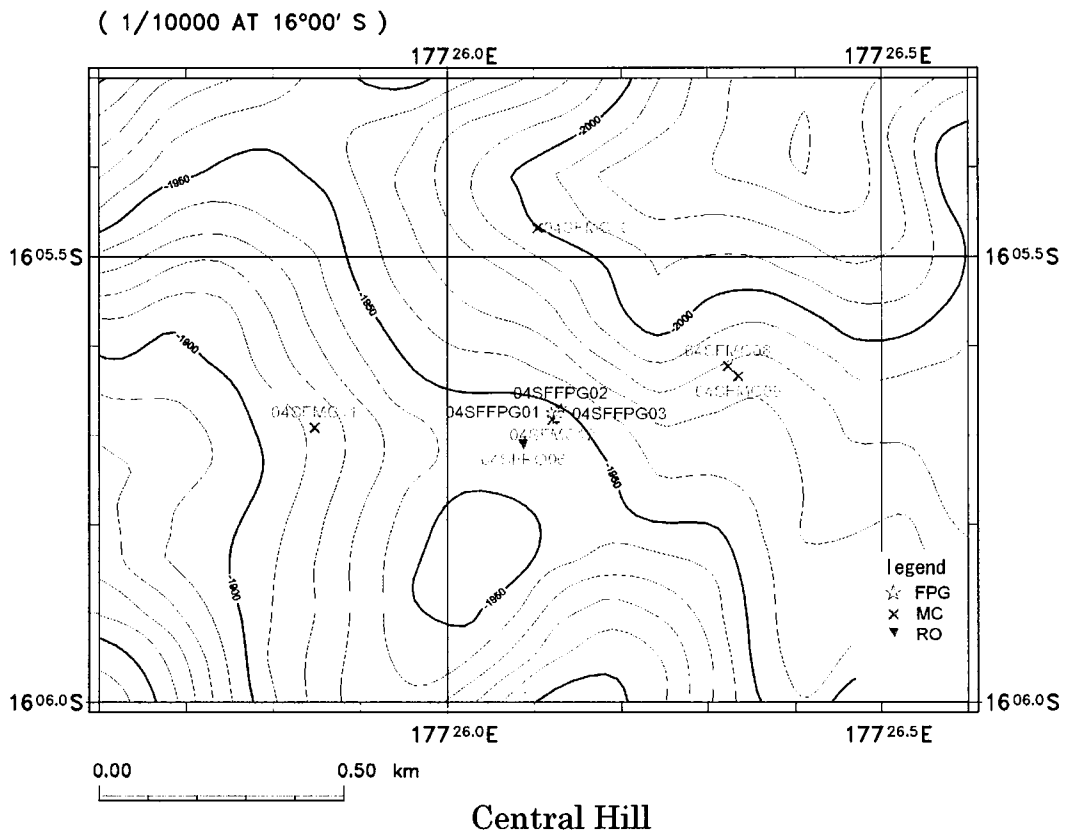
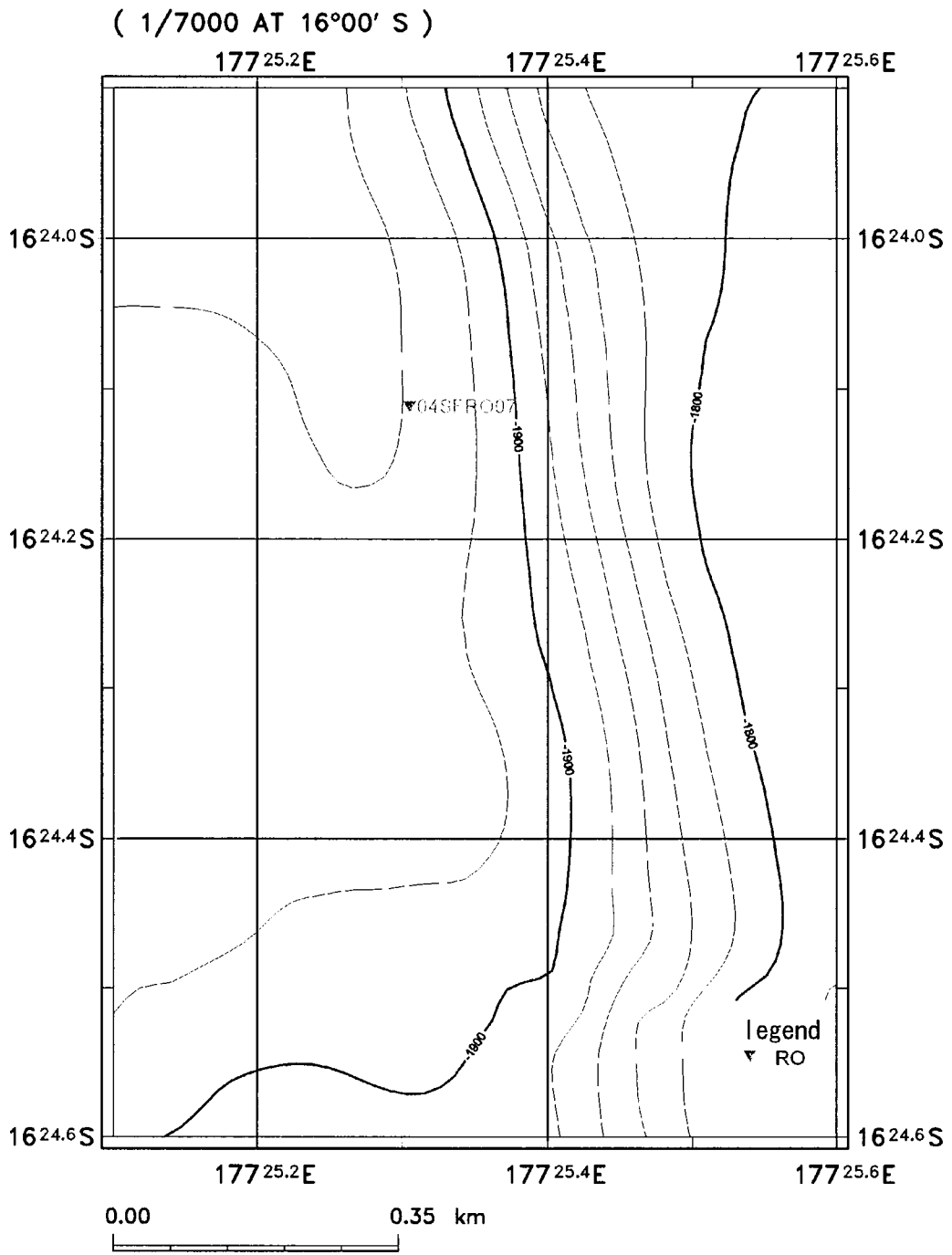


Figure 4 - 1 - 1 Survey stations (1)



ERZ A

Figure 4 - 1 - 2 Survey stations (2)

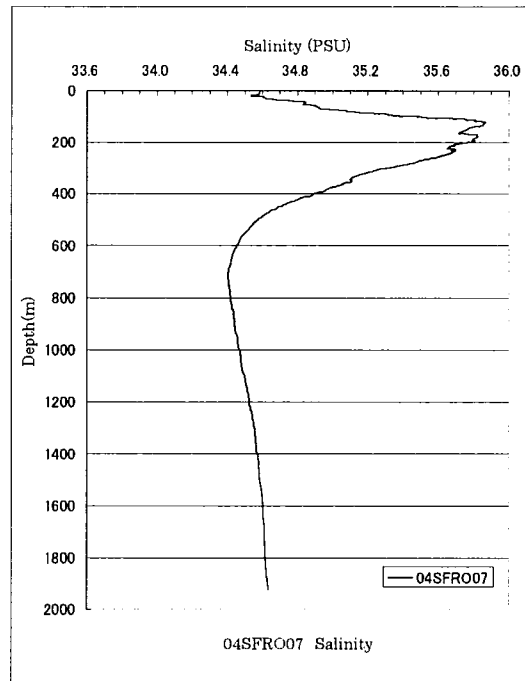
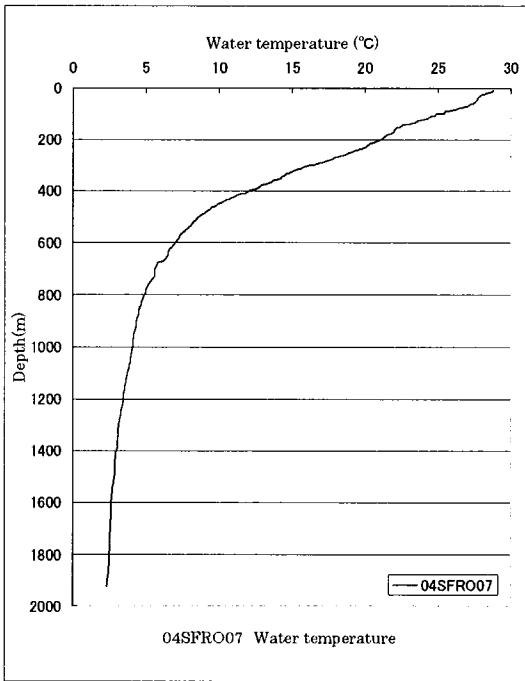
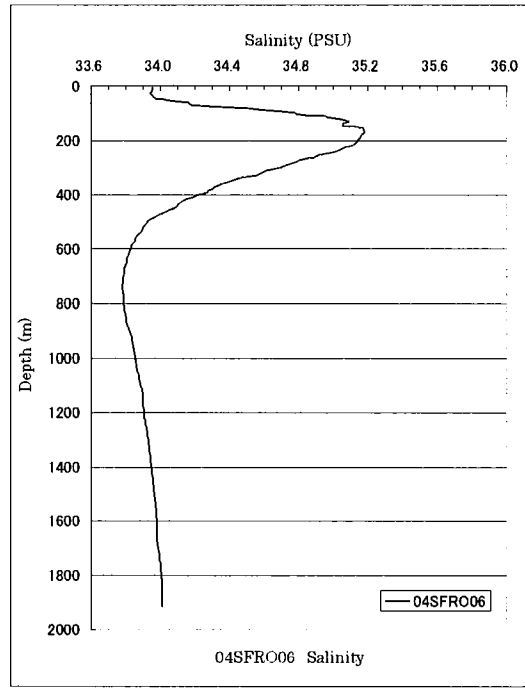
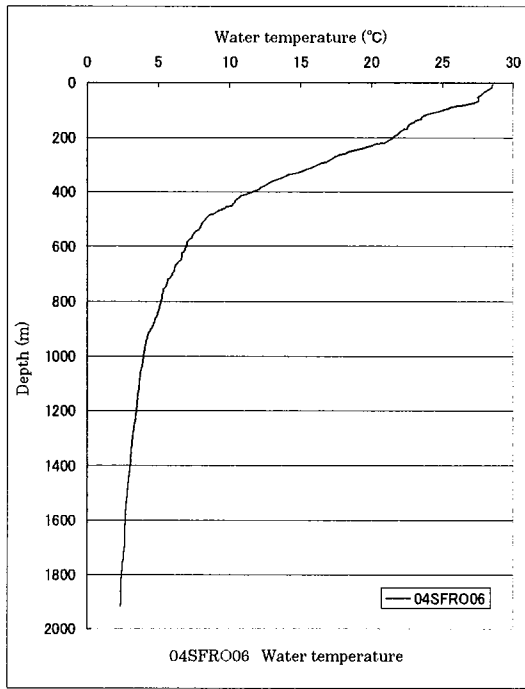


Figure 4 - 2 - 1 Vertical profiles of water temperature and salinity

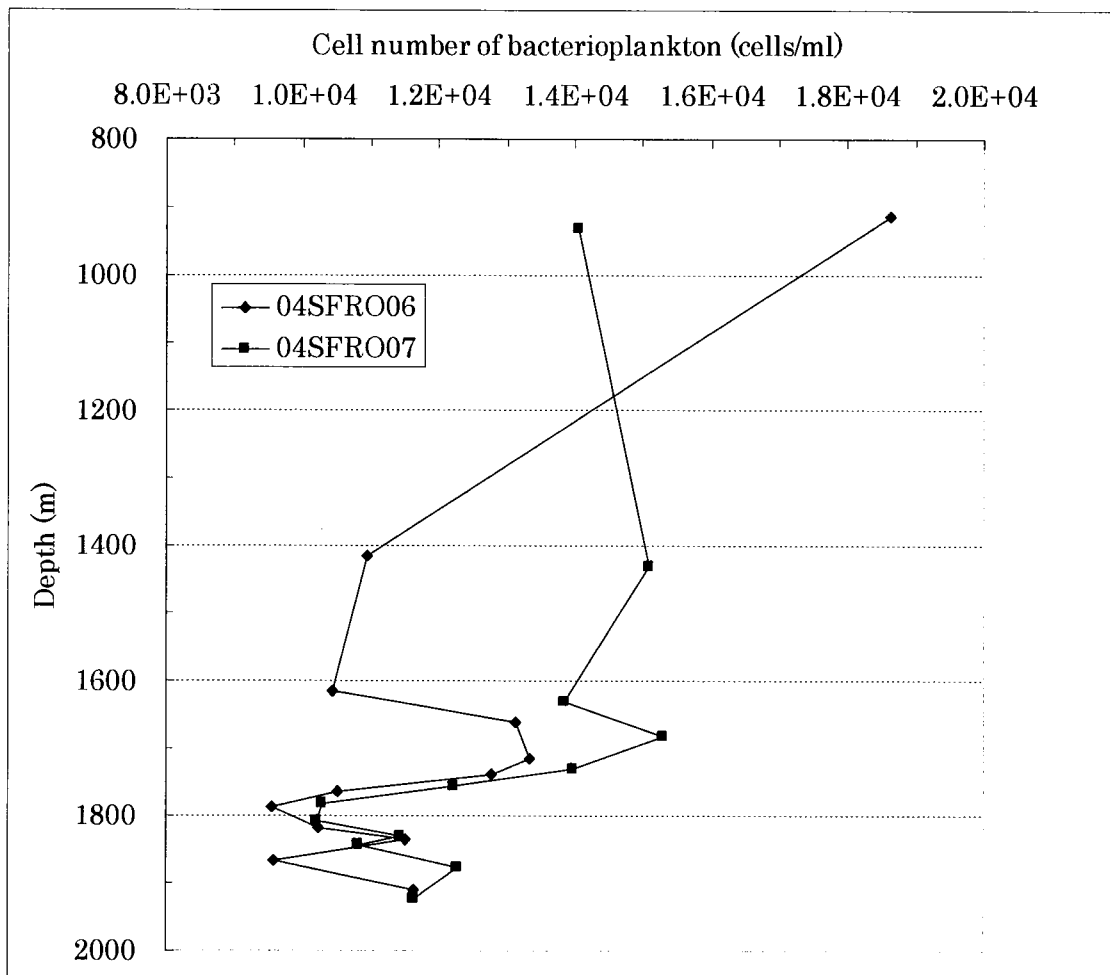


Figure 4 - 2 - 2 Distribution of bacterioplankton

#### 4-2-3 Summary

A T-S diagram of depths below 1,400 m was prepared to confirm hydrothermal plumes for both station (Figures 4-2-3 and 4-2-4). Regression lines between water temperature and salinity from 1,400 m to 1,600 m and data measured at depths of 1,400 meters and deeper were drawn. Both stations belong to low water temperature and high salinity regions. Both stations showed a shift towards the direction having the higher value toward the sea bed as estimated from the regression formula of water temperature and salinity. The difference for each depth between water temperature and the value found using the regression formula is shown in Figure 4-2-5. This result showed that below 1,600 m the difference was large implying that there is water temperature abnormality at this depth. In addition, the depth exhibiting temperature abnormality corresponded to the layer in which bacterial cell number was increased.

Generally, it may be thought that plumes form in the vicinity of the survey sea area due to the release of thermal water that caused the existence anomalous water temperature toward the sea bed. This phenomenon also may have caused the increase in the number of bacteria assumed to be utilizing the chemical components of the plumes as energy source. Further investigation on the activities of manganese, methane and other chemical components as an indicator of hydrothermal activity, is suggested.



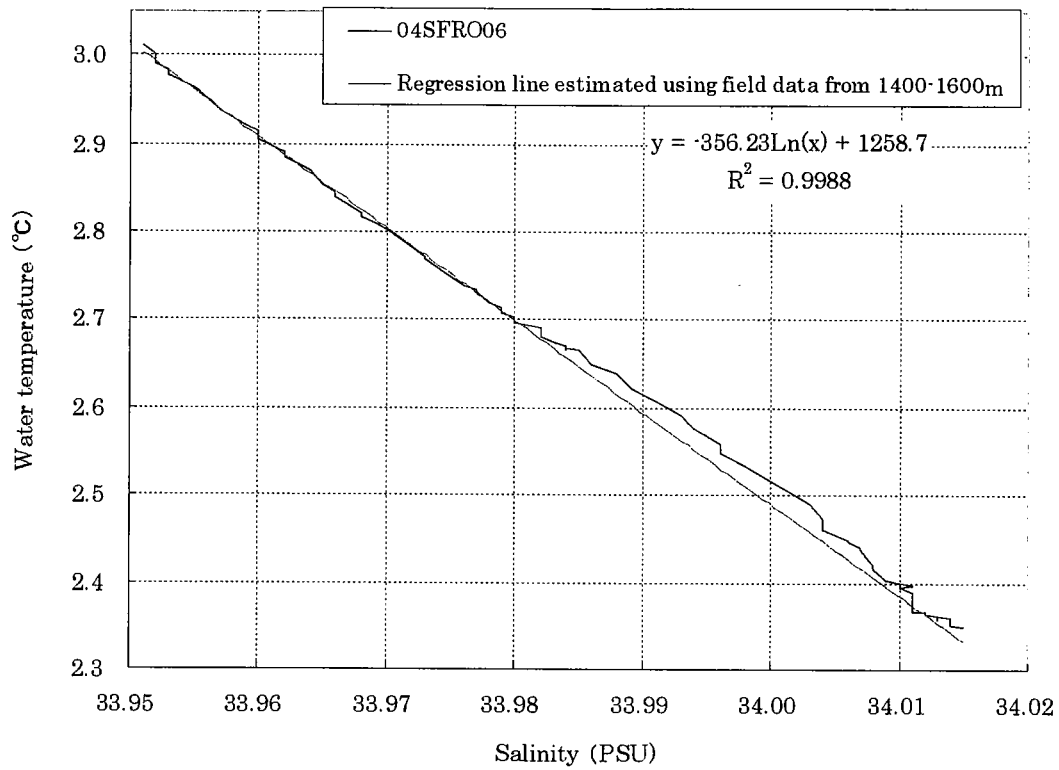


Figure 4 - 2 - 3 T/S diagram below 1400m depth at 04SFRO06 and regression line estimated using field data from 1400-1600m

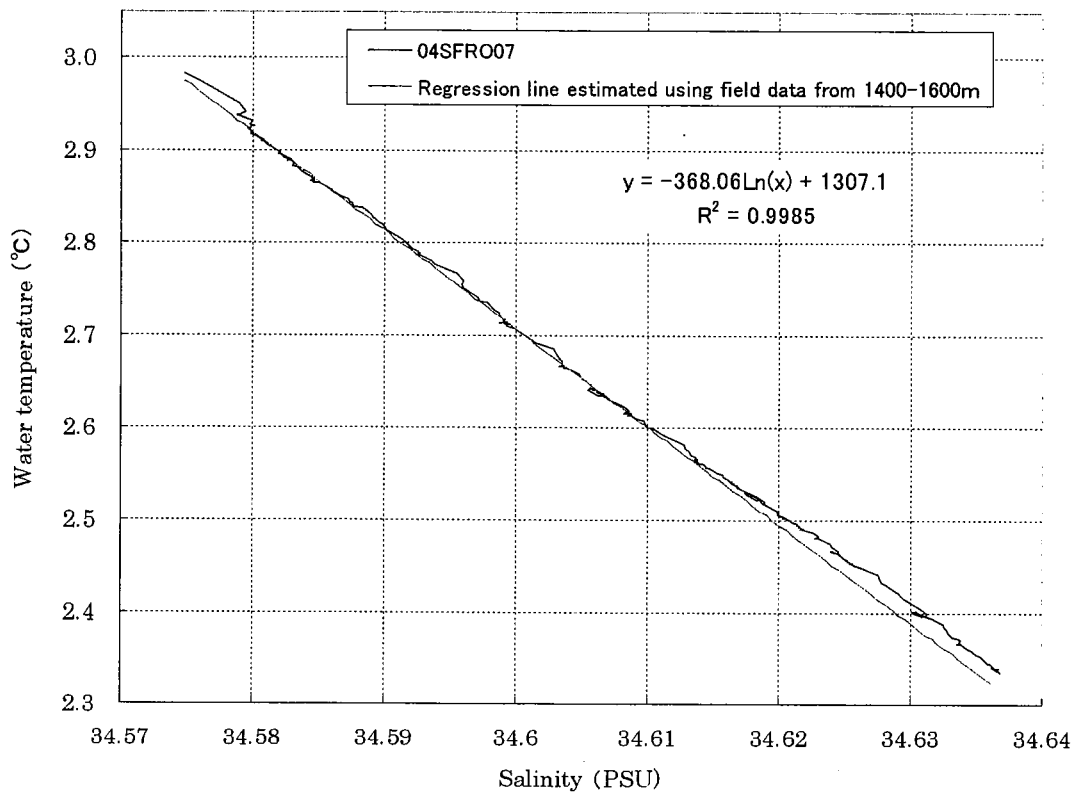
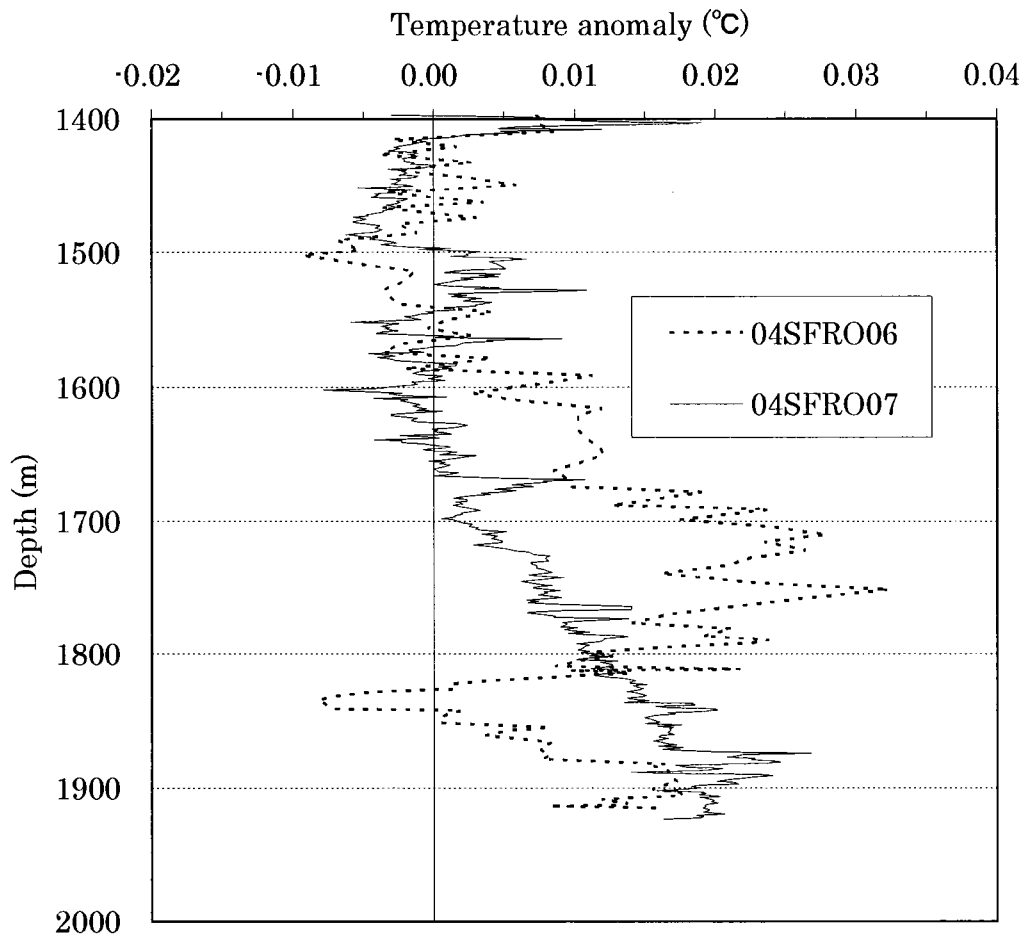


Figure 4 - 2 - 4 T/S diagram below 1400m depth at 04SFRO07 and regression line estimated using field data from 1400-1600m



**Figure 4 - 2 - 5 Vertical profile of water temperature anomaly. Water temperature anomaly is derived as the difference between field data and estimated data using equations shown in Figure 4-2-3 and 4-2-4**

### 4-3 Bottom Sediment and Benthic Organism

#### 4-3-1 Bottom Sediment

##### (1) Water Content

The vertical distributions of the water content at each station were shown in Figure 4-3-1 and Table 2. At 04SFMC09, the average water content was 53.2% from the surface to 1 cm layer, and 47.2-48.9% in depths greater than 1 cm. At 04SFMC10, the value was 54.9% on average in the 0-1 cm layer, and 47.3-50.7% deeper than 1 cm depth. At 04SFMC11, the water content was 51.0% in the 0-1 cm layer showing a tendency to decrease from the 1 cm depth to the deeper layers, and the minimum value was 43.9% in the 7-8 cm layer.

At 04SFMC09 and 04SFMC10, the water content was higher in 0-1 cm layer, and showed lower value in the layers between 3 and 5 cm; it increased slightly below 5 cm. At 04SFMC11, however, the water content decreased from the surface to the 8 cm.

##### (2) Calcium Carbonate (CaCO<sub>3</sub>)

The vertical distributions of calcium carbonate at each station were shown in Figure 4-3-1 and Table 2. At 04SFMC09, the minimum value for calcium carbonate was 70.2% on average in the 1-2 cm layer, and the maximum value was 77.6% on average in the 6-7 cm and 7-8 cm layers. At 04SFMC10, the minimum value for calcium carbonate was 71.2% on average in the 0-1 cm layer, and the maximum value was 83.2% on average in the 7-8 cm layer. At 04SFMC11, the minimum value for calcium carbonate was 78.3% on average in the 0-1 cm layer, and the maximum value was 94.1% on average in the 5-6 cm layer.

At 04SFMC09 and 04SFMC10, the concentrations of calcium carbonate showed the tendency to increase from the surface to deeper layers. However, the concentrations of calcium carbonate at 04SFMC11 were higher in all the layers than at the other two stations, and there was the greatest value at the 5-6 cm layer.

##### (3) Total Organic Carbon (TOC)

The vertical distributions of the total organic carbon at each station were shown in Figure 4-3-1 and Table 2. At 04SFMC09, the concentration of total organic carbon was 1.85 mg/g-dry on average in the 0-1 cm layer and 1.32 -1.61 mg/g-dry on average in the deeper than 1 cm depth. At 04SFMC10, the total organic carbon was 2.04 mg/g-dry on average in the 0-1 cm layer and 1.43-1.84 mg/g-dry in the deeper than 1 cm depth. At 04SFMC11, the maximum value of total organic carbon was 1.93 mg/g-dry in the 2-3

cm layer, and the minimum value was 1.22 mg/g-dry in the 5-6 cm layer.

At 04SFMC09 and 04SFMC10, the concentrations of total organic carbon were highest in the 0-1 cm layer, and only a little variation was observed deeper than 1 cm depth vertically. However, at 04SFMC11, the concentrations were higher in the layers between 0 to 3 cm and significantly lower in the layers between 4 to 8 cm.

#### (4) Total Nitrogen (T-N)

The vertical distributions of total nitrogen at each station were shown in Figure 4-3-1 and Table 2. At 04SFMC09, the concentrations of total nitrogen were between 0.21 -0.30 mg/g-dry on average and only a little variation was observed vertically. At 04SFMC10, the concentration was 0.33 mg/g-dry on average in the 0-1 cm layer, and 0.23-0.27 mg/g-dry and stable deeper than 1 cm depth. At 04SFMC11, the maximum value was 0.40 mg/g-dry on average in the 2-3 cm layer, and the minimum value was 0.24 mg/g-dry, in the 5-6 cm layer. Both the total nitrogen and total organic carbon were higher at the surface layer and significantly lower in the deeper layers. The maximum value of total organic carbon was 1.93 mg/g-dry in the 2-3 cm layer, and the minimum value was 1.22 mg/g-dry in the 5-6 cm layer.

#### (5) Total Sulfide (T-S)

The concentrations of total sulfide were below the detection limit in all the samples at all the stations (Table 2).

#### (6) Specific Gravity

The vertical distributions of the specific gravity at each station were shown in Figure 4-3-1 and Table 2. At 04SFMC09, the specific gravity values were 2.75-2.79 on average in all the layers. Similarly, at 04SFMC10, the specific gravity values were 2.76-2.78 on average in all the layers. At 04SFMC11, the lowest value was 2.74 in the 0-1 cm layer, and the highest was 2.83 in the 7-8 cm layer.

#### (7) The correlation between measurements for the bottom sediment

The correlation between measurements for the bottom sediment is shown in Figure 4-3-2, and the correlation matrix is shown in Table 4-3-1. The strong correlation was observed between the water content and the total organic carbon as well as between total organic carbon and total nitrogen. The correlation coefficients were 0.69 and 0.57, respectively. No correlations were found among other properties.

**Table 4 - 3 - 1 Correlation matrix of sediment properties**

Properties	Water content	CaCO <sub>3</sub>	TOC	T-N	Specific gravity
Water content	1.00				
CaCO <sub>3</sub>	-0.47	1.00			
TOC	0.69	-0.29	1.00		
T-N	0.26	0.21	0.57	1.00	
Specific gravity	-0.20	0.31	-0.23	-0.18	1.00

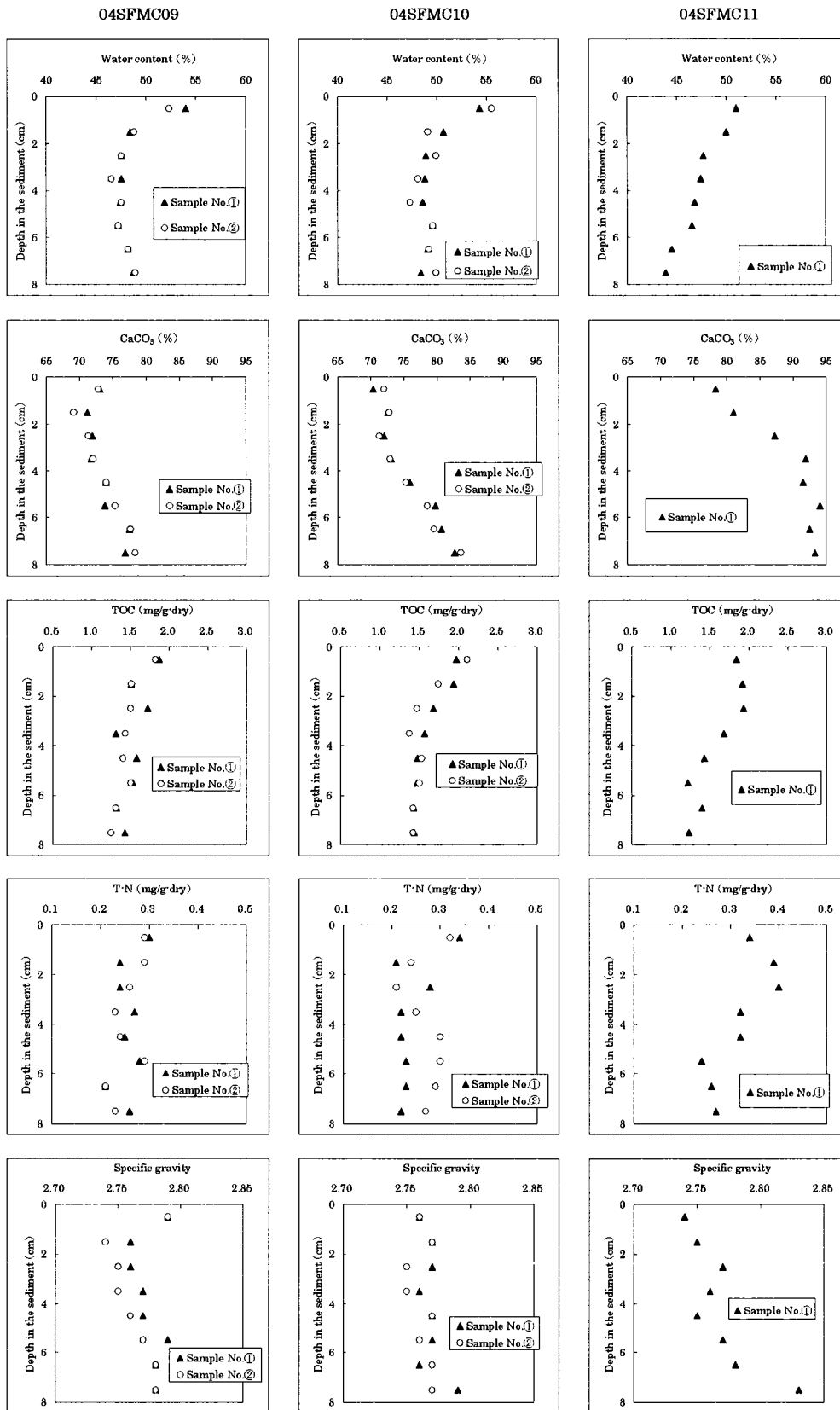


Figure 4 - 3 - 1 Vertical profiles of sediment properties

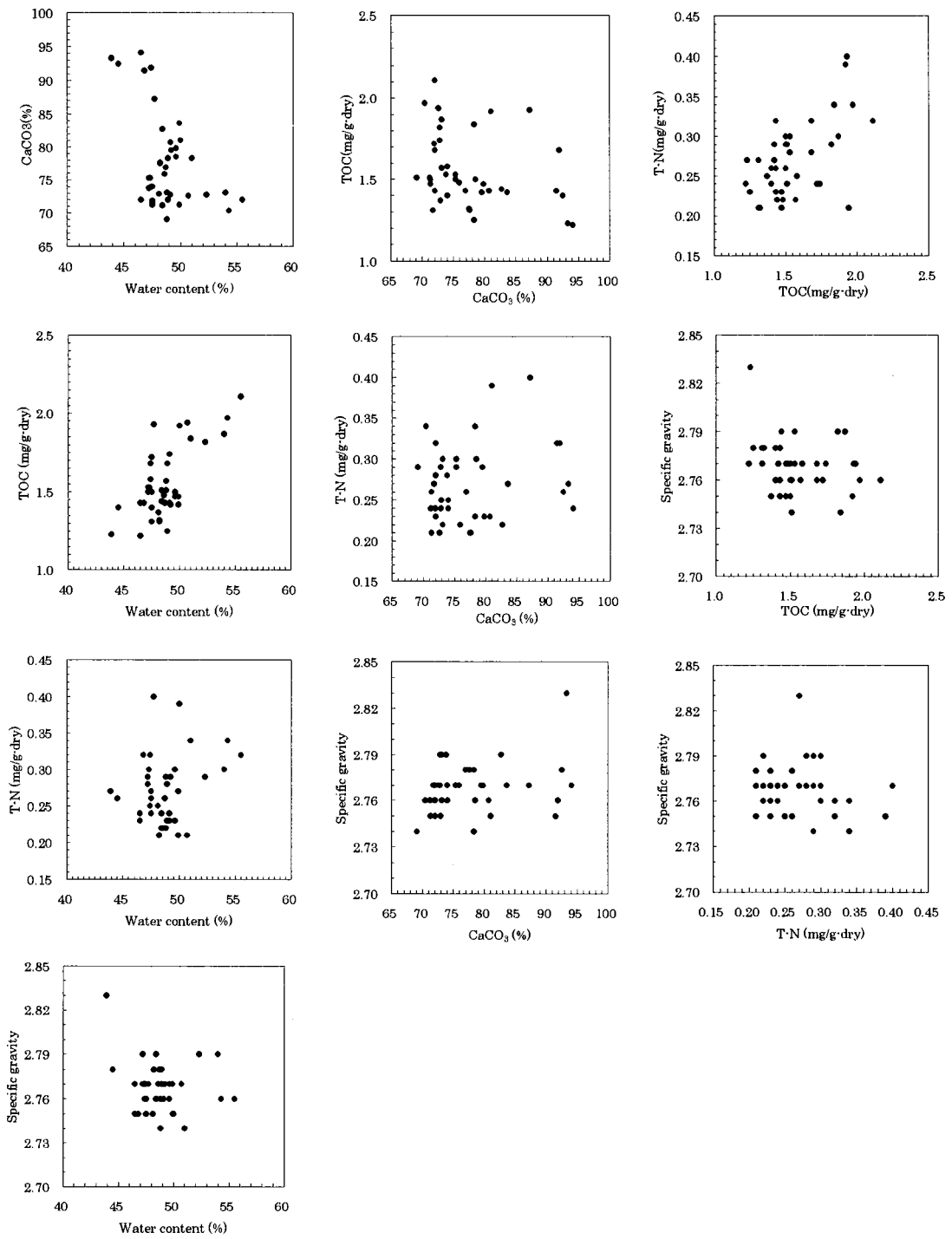


Figure 4 - 3 - 2 Relationship among sediment properties

## 4-3-2 Benthic Organisms

### (1) Sedimentary Bacteria

The vertical distributions of abundances on sedimentary bacteria at each station were shown in Figure 4-3-3 and Table 3. At 04SFMC09, the highest abundance was  $1.84 \times 10^8$  cells/g-dry on average in the 0-1 cm layer, and in layers deeper than 1 cm, the abundances were between  $2.25 \times 10^7$  and  $6.78 \times 10^7$  cells/g-dry on average. At 04SFMC10, the highest abundance was  $1.02 \times 10^8$  cells/g-dry on average in the 0-1 cm layer, and the abundances decreased in 0-1 cm and 4-5 cm layers, and increased slightly in the 5-6 cm layer. At 04SFMC11, the highest abundance was  $2.74 \times 10^8$  cells/g-dry in the 0-1 cm layer, and increased in 5-6 cm layer similarly to 04SFMC10.

At all stations, there were the highest abundances in the 0-1 cm layer, and showed a slight increase in the 5-6 cm layer. The abundances were higher in all the layers at 04SFMC11 than those of the other two stations.

### (2) Meiobenthos

Eleven taxa were identified in the meiobenthos samples, including the phyla Protozoa (Foraminiferida), Nematoda (two taxa), Kinorhyncha, Loricifera, Tradigrada, Annelidia (Polychaeta) and Arthropoda (Ostracoda, Harpacticoida, Copepoda, and Nauplius larva) (Table 4-3-2). Foraminiferida, Nematoda, Harpacticoida and Nauplius larva were found at all the stations.

The average of the total meiobenthos abundances were 381.6 inds./10 cm<sup>2</sup> at 04SFMC09, 282.6 inds./10 cm<sup>2</sup> at 04SFMC10, and 580.6 inds./10 cm<sup>2</sup> at 04SFMC11; 04SFMC11 gave a higher number than the other two stations (Figure 4-3-4). Nematoda accounted for at least 64% at all stations, and 78% at 04SFMC11. Foraminiferida accounted for at least 18% at all the stations.

The vertical distributions at 04SFMC09 and 04SFMC10 indicated that the number of meiobenthos was highest in the 0-1 cm layer, and accounted for at least 64% (Figure 4-3-5). At 04SFMC11, many meiobenthos were found at depths of 0-1 cm, 1-2 cm, and 4-5 cm, and accounted for 38%, 18%, and 17% respectively at those depths.

Meiobenthos abundances correlated with water content, total organic carbon, and total nitrogen, and the correlation coefficients were 0.68, 0.65, and 0.50 respectively (Figure 4-3-6, Table 4-3-3). Meiobenthos did not correlate with calcium carbonate and specific gravity.



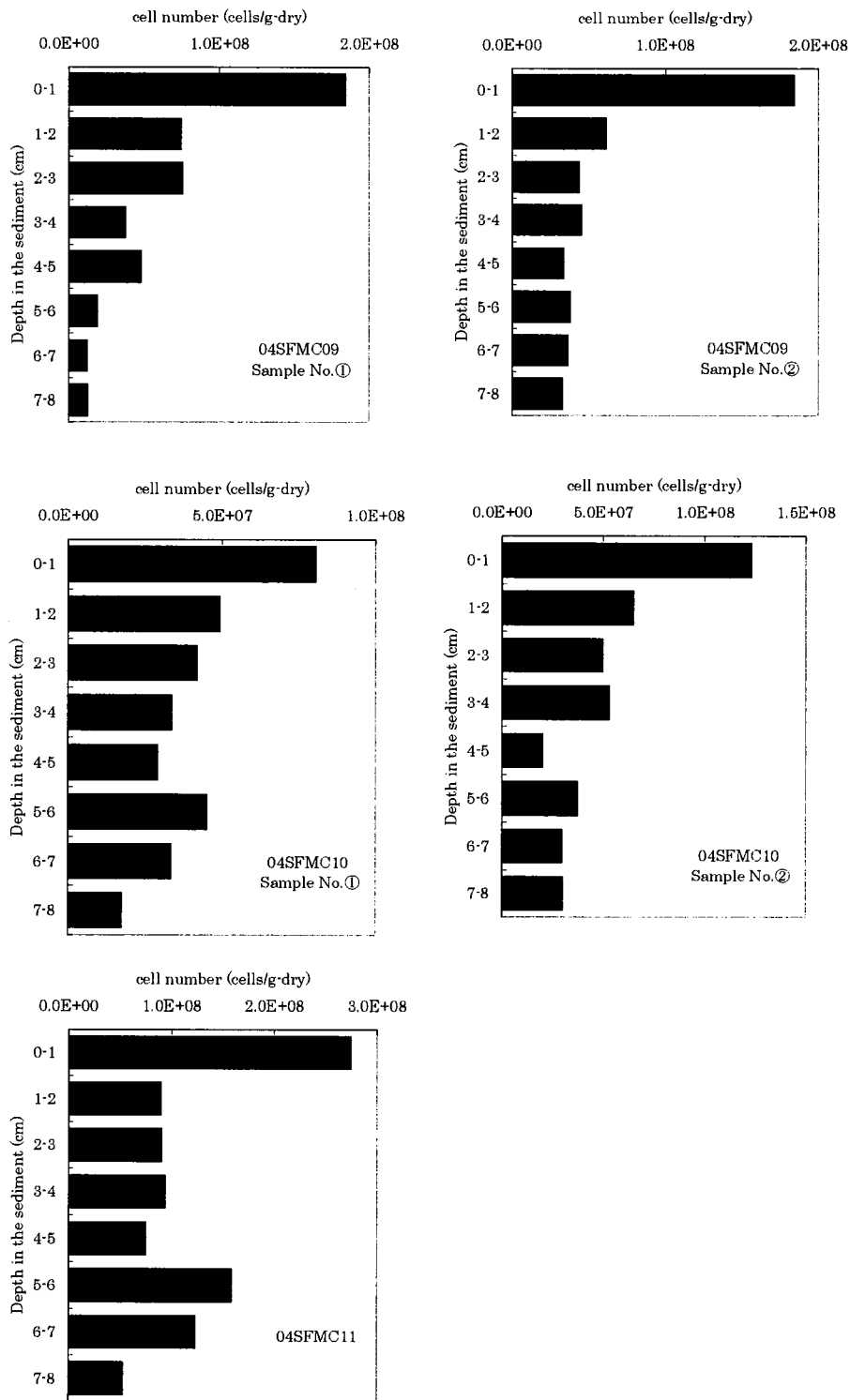


**Figure 4 - 3 - 3 Vertical profiles of sedimentary bacteria**

Table 4 - 3 - 2 Species and abundance of meiobenthos at each station

unit: inds./10cm<sup>3</sup>

No.	Taxa	04SFM09 ①								total
		(cm)								
		0-1	1-2	2-3	3-4	4-5	5-6	6-7	7-8	
1	Foraminiferida	76.7	9.0	6.8	6.8	4.5				103.8
2	NEMATODA	180.6	49.7	15.8	11.3	22.6	11.3		2.3	293.6
3	NEMATODA (Desmoscolecidae)	13.5								13.5
4	KINORHYNCHA	2.3								2.3
5	LORICIFERA									0.0
6	TARDIGRADA									0.0
7	Polychaeta									0.0
8	Ostracoda	2.3								2.3
9	Harpacticoida	4.5								4.5
10	Copepoda									0.0
11	Nauplius	9.0								9.0
	total	288.9	58.7	22.6	18.1	27.1	11.3	0.0	2.3	429.0

No.	Taxa	04SFM09 ②								total
		(cm)								
		0-1	1-2	2-3	3-4	4-5	5-6	6-7	7-8	
1	Foraminiferida	72.2	2.3	9.0					2.3	85.8
2	NEMATODA	126.4	29.3	13.5	6.8	13.5	4.5	9.0	4.5	207.5
3	NEMATODA (Desmoscolecidae)	22.6								22.6
4	KINORHYNCHA	2.3								2.3
5	LORICIFERA									0.0
6	TARDIGRADA									0.0
7	Polychaeta	2.3								2.3
8	Ostracoda									0.0
9	Harpacticoida	6.8								6.8
10	Copepoda									0.0
11	Nauplius	6.8								6.8
	total	289.4	31.6	22.5	6.8	13.5	4.5	9.0	6.8	334.1

No.	Taxa	04SFM10 ①								total
		(cm)								
		0-1	1-2	2-3	3-4	4-5	5-6	6-7	7-8	
1	Foraminiferida	54.2	9.0					2.3	2.3	67.8
2	NEMATODA	103.8	40.6	13.5	4.5	2.3	4.5		2.3	171.5
3	NEMATODA (Desmoscolecidae)	6.8	2.3	2.3	2.3					13.7
4	KINORHYNCHA									0.0
5	LORICIFERA									0.0
6	TARDIGRADA									0.0
7	Polychaeta	2.3								2.3
8	Ostracoda	2.3								2.3
9	Harpacticoida	2.3								2.3
10	Copepoda	2.3								2.3
11	Nauplius	11.3	2.3							13.6
	total	185.3	54.2	15.8	6.8	2.3	4.5	2.3	4.6	275.8

No.	Taxa	04SFM10 ②								total
		(cm)								
		0-1	1-2	2-3	3-4	4-5	5-6	6-7	7-8	
1	Foraminiferida	70.0	9.0	6.8				2.3	2.3	90.4
2	NEMATODA	97.1	33.9	9.0	6.8	11.3	2.3	4.5	4.5	169.4
3	NEMATODA (Desmoscolecidae)	11.3	4.5		2.3					18.1
4	KINORHYNCHA									0.0
5	LORICIFERA									0.0
6	TARDIGRADA	2.3								2.3
7	Polychaeta									0.0
8	Ostracoda									0.0
9	Harpacticoida	4.5								4.5
10	Copepoda									0.0
11	Nauplius	2.3		2.3						4.6
	total	187.5	47.4	18.1	9.1	11.3	2.3	6.8	6.8	289.3

No.	Taxa	04SFM11								total
		(cm)								
		0-1	1-2	2-3	3-4	4-5	5-6	6-7	7-8	
1	Foraminiferida	60.9	20.3	4.5	6.8	9.0	2.3	2.3		106.1
2	NEMATODA	117.4	81.3	18.1	45.1	88.0	42.9	27.1	2.3	422.2
3	NEMATODA (Desmoscolecidae)	22.6	2.3	2.3		2.3				29.5
4	KINORHYNCHA									0.0
5	LORICIFERA	2.3								2.3
6	TARDIGRADA						2.3			2.3
7	Polychaeta	2.3								2.3
8	Ostracoda	2.3								2.3
9	Harpacticoida	6.8	2.3							9.1
10	Copepoda									0.0
11	Nauplius	4.5								4.5
	total	219.1	106.2	24.9	51.9	99.3	47.5	29.4	2.3	580.6

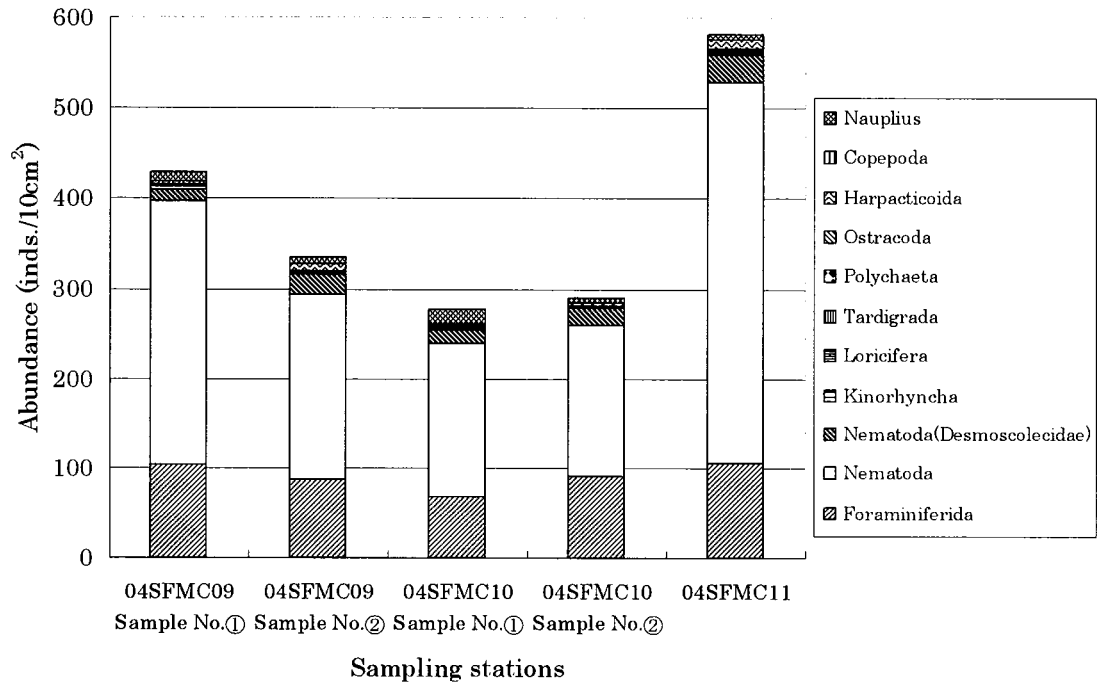
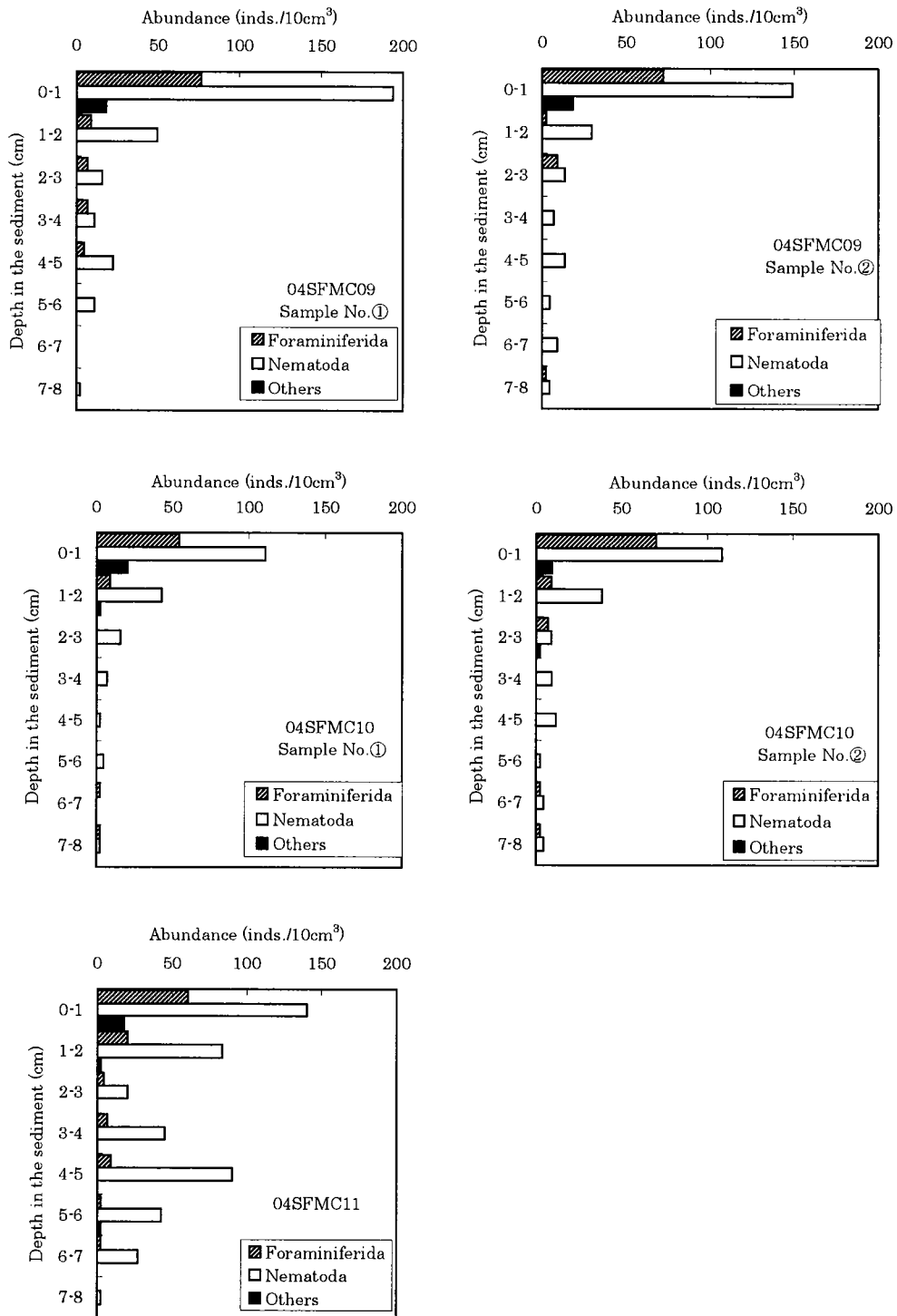
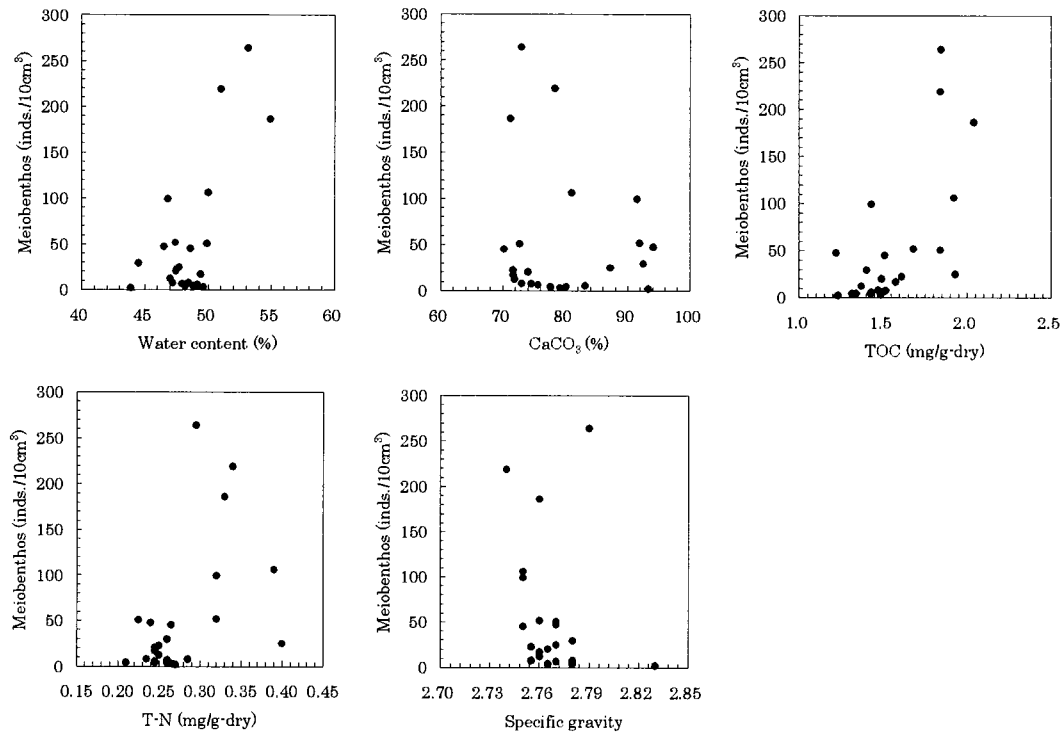


Figure 4 - 3 - 4 Abundances of meiobenthos at each station



**Figure 4 - 3 - 5 Vertical profiles of meiobenthos at each station**  
 \*Abundance of Nematoda in this figure is the sum of that of 「Nematoda」 and 「Nematoda (Desmoscolecidae)」 in Table 4-3-2



**Figure 4 - 3 - 6 Correlation between meiobenthos and sediment properties**


**Table 4 - 3 - 3 Correlation matrix of meiobenthos abundance and sediment properties**

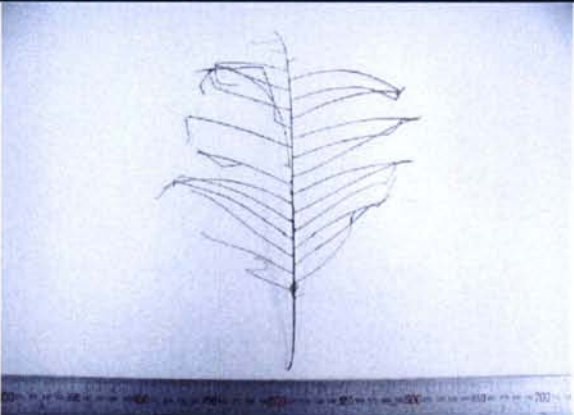
Properties	Water content	CaCO <sub>3</sub>	TOC	T-N	Specific gravity
Meiobenthos (inds./10cm <sup>3</sup> )	0.68	-0.12	0.65	0.50	-0.22


### (3) Macrobenthos

Macrobenthos organisms were obtained using FPG and AD, however, these surveys were not quantitative. Many macrobenthos were obtained using FPG, and few were obtained using AD (Table 4-3-4). Sixteen taxa were identified in the macrobenthos samples, including the phyla Porifera, Cnidaria (three taxa), Annelidia (three taxa) Vestimentifera, Mollusca (five taxa) and Arthropoda (three taxa). Figure 4-3-7 shows images of collected macrobenthos organisms. Vestimentifera and *Bathymodiolus* sp. were collected at 04SFFPG01, and Vestimentifera, *Calyptogena* sp. were collected at 04SFFPG03. These macrobenthos organisms which characterize chemotrophic community derived of hydrothermal deposits



Phylum	cf. PORIFERA	
_____ scale: 1mm		

Phylum	CNIDARIA	
Class	HYDROZOA	
Order	Hydroida	
Family	Plumulariidae	
	<b>Plumulariidae</b>	
_____ scale: 1mm		

Phylum	ANNELIDA	
Class	POLYCHAETA	
Order	Phyllodocida	
Family	Polynoidae	
	<i>Branchipolynoe pettiboneae</i>	
_____ scale: 1mm		


Phylum	ANNELIDA	
Class	POLYCHAETA	
Order	Phyllodocida	
Family	Nereididae	
	<b>Nereididae</b>	
_____ scale: 1mm		

Figure 4 - 3 - 7 (1) Images of collected macrobenthos





Phylum	MOLLUSCA
Class	BIVALVIA
Order	Veneroida
Family	Lucinidae
	<i>Lucinoma</i> sp.



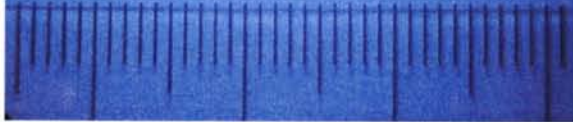
scale:1mm



Phylum	ARTHROPODA
Class	CRUSTACEA
Order	Thecostraca
Family	Scalpellidae
	<b>Scalpellidae</b>



scale:1mm



Phylum	ARTHROPODA
Class	CRUSTACEA
Order	Thecostraca
Family	Balanidae
	<b>Balanidae</b>



scale:1mm



Phylum	ARTHROPODA
Class	CRUSTACEA
Order	Decapoda
Family	Galatheidae
	<i>Munidopsis</i> sp.



scale:1mm

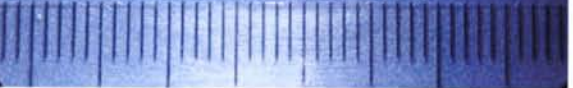


Figure 4 - 3 - 7 (3) Images of collected macrobenthos

#### 4-3-3 Summary

Sediment properties were compared between the sampling stations. The vertical distribution of water content, calcium carbonate, organic carbon, total nitrogen and specific gravity at 04SFMC09 and 04SFMC10 were analogous. However, vertical distributions of these parameters differed at 04SFMC11. In particular, the concentrations of calcium carbonate were highest in the 5-6 cm layer compared with the other two stations. Calcium carbonate is deposited in the sediment as ejection of thermal water from the plumes progresses. The higher calcium carbonate content in the sediments of 04SFMC11 suggests hydrothermal deposits in this area.

The abundances of sedimentary bacteria and meiobenthos were also much higher in 04SFMC11 than 04SFMC09 or 04SFMC10.

The results of macrobenthos survey cannot be compared with the results from the sediment properties obtained from the sedimentary bacteria and the meiobenthos survey because the collection method and survey stations for the macrobenthos survey were different from those of the other subjects. However, analysis of the macrobenthos revealed a number of chemotrophic organisms, such as tube-dwelling worms (*Vestimentifera*) and bivalves (*Calyplogena* sp. etc.) at 04SFFPG01 and 04SFFPG03.

Comparing the correlations between the abundance of meiobenthos and each sediment properties, better correlation was observed with the organic carbon. This result could probably imply that the meiobenthos are utilizing organic carbon in the bottom sediment as food.

## **5. Conclusion**

The environmental survey was carried out in designated areas as a baseline study to evaluate the magnitude of mining impacts on deep-sea environment. The survey was done to understand: 1) the water quality/ bacterioplankton survey and 2) the bottom sediment and benthic organism survey.

Results of the water quality and sedimentary bacteria survey, confirms the existence of an abnormal distribution of water temperature and bacteria in water depths greater than 1,600 m. This finding supports the possibility that hydrothermal plumes were present in these areas. In the survey of sediment properties and benthic organism, higher concentrations of calcium carbonate in 04SFMC11 than in 04SFMC09 and 04SFMC10 suggests that 04SFMC11 is affected by the hydrothermal deposits accumulated from the activity of thermal water. The presence of hydrothermal deposits is further supported by the observation of a number of chemotrophic macrobenthos, such as tube-dwelling worms and bivalves at 04SFFPG01 and 04SFFPG03.

Generally, these findings lead to a conclusion that effects of hydrothermal activity were recognized in the survey areas. Further investigation on the activities of manganese, methane and other chemical components as an indicator of hydrothermal activity, is suggested.

### Appendix 1 Analytical results for bacterioplankton

Station	Sample No.	Depth (m)	Cell number (cells/ml)
04SFRO06	1	1910	1.16E+04
	2	1866	9.57E+03
	3	1837	1.15E+04
	4	1817	1.02E+04
	5	1787	9.55E+03
	6	1764	1.05E+04
	7	1739	1.28E+04
	8	1716	1.33E+04
	9	1662	1.31E+04
	10	1616	1.04E+04
	11	1415	1.10E+04
	12	914	1.86E+04
04SFRO07	1	1922	1.16E+04
	2	1878	1.23E+04
	3	1844	1.08E+04
	4	1830	1.14E+04
	5	1806	1.02E+04
	6	1782	1.03E+04
	7	1756	1.22E+04
	8	1732	1.40E+04
	9	1681	1.53E+04
	10	1631	1.39E+04
	11	1431	1.51E+04
	12	932	1.40E+04

### Appendix 2 Analytical results for sediment properties

Station	Sample No.	Layer (cm)	Water content (%)	CaCO <sub>3</sub> (%)	TOC (mg/g-dry)	T-N (mg/g-dry)	T-S (mg/g-dry)	Specific gravity
04SFMC09	①	0-1	54.0	73.1	1.87	0.30	<0.01	2.79
		1-2	48.4	71.2	1.51	0.24	<0.01	2.76
		2-3	47.5	71.9	1.72	0.24	<0.01	2.76
		3-4	47.5	71.7	1.31	0.27	<0.01	2.77
		4-5	47.4	74.0	1.58	0.25	<0.01	2.77
		5-6	47.2	73.8	1.53	0.28	<0.01	2.79
		6-7	48.2	77.5	1.32	0.21	<0.01	2.78
		7-8	48.7	76.9	1.43	0.26	<0.01	2.78
	②	0-1	52.3	72.8	1.82	0.29	—	2.79
		1-2	48.8	69.1	1.51	0.29	—	2.74
		2-3	47.5	71.3	1.50	0.26	—	2.75
		3-4	46.5	72.0	1.43	0.23	—	2.75
		4-5	47.5	74.0	1.40	0.24	—	2.76
		5-6	47.2	75.3	1.50	0.29	—	2.77
		6-7	48.2	77.6	1.31	0.21	—	2.78
		7-8	48.9	78.3	1.25	0.23	—	2.78
04SFMC10	①	0-1	54.3	70.4	1.97	0.34	<0.01	2.76
		1-2	50.7	72.6	1.94	0.21	<0.01	2.77
		2-3	48.9	72.0	1.68	0.28	<0.01	2.77
		3-4	48.8	73.1	1.57	0.22	<0.01	2.76
		4-5	48.6	75.9	1.48	0.22	<0.01	2.77
		5-6	49.6	79.8	1.47	0.23	<0.01	2.77
		6-7	49.1	80.7	1.43	0.23	<0.01	2.76
		7-8	48.4	82.7	1.44	0.22	<0.01	2.79
	②	0-1	55.5	72.0	2.11	0.32	—	2.76
		1-2	49.1	72.8	1.74	0.24	—	2.77
		2-3	49.9	71.3	1.47	0.21	—	2.75
		3-4	48.1	72.9	1.37	0.25	—	2.75
		4-5	47.3	75.3	1.53	0.30	—	2.77
		5-6	49.6	78.5	1.50	0.30	—	2.76
		6-7	49.2	79.5	1.42	0.29	—	2.77
		7-8	49.9	83.6	1.42	0.27	—	2.77
04SFMC11	①	0-1	51.0	78.3	1.84	0.34	<0.01	2.74
		1-2	50.0	81.0	1.92	0.39	<0.01	2.75
		2-3	47.7	87.2	1.93	0.40	<0.01	2.77
		3-4	47.4	91.9	1.68	0.32	<0.01	2.76
		4-5	46.8	91.5	1.43	0.32	<0.01	2.75
		5-6	46.5	94.1	1.22	0.24	<0.01	2.77
		6-7	44.5	92.5	1.40	0.26	<0.01	2.78
		7-8	43.9	93.3	1.23	0.27	<0.01	2.83

**Appendix 3 Analytical results for sedimentary bacteria**

Station	Sample No.	Layer (cm)	Cell number (cells/g·dry)
04SFMC09	①	0-1	1.84E+08
		1-2	7.43E+07
		2-3	7.53E+07
		3-4	3.75E+07
		4-5	4.78E+07
		5-6	1.89E+07
		6-7	1.20E+07
		7-8	1.25E+07
	②	0-1	1.84E+08
		1-2	6.14E+07
		2-3	4.36E+07
		3-4	4.52E+07
		4-5	3.35E+07
		5-6	3.78E+07
		6-7	3.61E+07
		7-8	3.26E+07
04SFMC10	①	0-1	8.04E+07
		1-2	4.92E+07
		2-3	4.17E+07
		3-4	3.35E+07
		4-5	2.90E+07
		5-6	4.51E+07
		6-7	3.32E+07
		7-8	1.71E+07
	②	0-1	1.23E+08
		1-2	6.47E+07
		2-3	4.94E+07
		3-4	5.29E+07
		4-5	2.00E+07
		5-6	3.72E+07
		6-7	2.94E+07
		7-8	2.96E+07
04SFMC11	①	0-1	2.74E+08
		1-2	8.91E+07
		2-3	8.98E+07
		3-4	9.35E+07
		4-5	7.47E+07
		5-6	1.58E+08
		6-7	1.23E+08
		7-8	5.23E+07